NUREG/IA-0401

International Agreement Report

Assessment of Two-Phase Critical Flow Models Performance in RELAP5 and TRACE Against Marviken Critical Flow Tests

Prepared by:
Lukasz Sokolowski
Tomasz Kozlowski

A. Calvo, NRC Project Manager

Office of Nuclear Regulatory Research
U.S. Nuclear Regulatory Commission
Washington, DC 20555-0001

Manuscript Completed: June 2011
Date Published: February 2012

Prepared as part of
The Agreement on Research Participation and Technical Exchange
Under the Thermal-Hydraulic Code Applications and Maintenance Program (CAMP)

Published by
U.S. Nuclear Regulatory Commission

AVAILABILITY OF REFERENCE MATERIALS IN NRC PUBLICATIONS

NRC Reference Material

As of November 1999, you may electronically access NUREG-series publications and other NRC records at NRC's Public Electronic Reading Room at http://www.nrc.gov/reading-rm.html. Publicly released records include, to name a few, NUREG-series publications; *Federal Register* notices; applicant, licensee, and vendor documents and correspondence; NRC correspondence and internal memoranda; bulletins and information notices; inspection and investigative reports; licensee event reports; and Commission papers and their attachments.

NRC publications in the NUREG series, NRC regulations, and *Title 10, Energy*, in the Code of *Federal Regulations* may also be purchased from one of these two sources.

1. The Superintendent of Documents
   U.S. Government Printing Office
   Mail Stop SSOP
   Washington, DC 20402–0001
   Internet: bookstore.gpo.gov
   Telephone: 202-512-1800
   Fax: 202-512-2250
2. The National Technical Information Service
   Springfield, VA 22161–0002
   www.ntis.gov
   1–800–553–6847 or, locally, 703–605–6000

A single copy of each NRC draft report for comment is available free, to the extent of supply, upon written request as follows:

Address: U.S. Nuclear Regulatory Commission
Office of Administration
Publications Branch
Washington, DC 20555-0001
E-mail: DISTRIBUTION.RESOURCE@NRC.GOV
Facsimile: 301–415–2289

Some publications in the NUREG series that are posted at NRC's Web site address http://www.nrc.gov/reading-rm/doc-collections/nuregs are updated periodically and may differ from the last printed version. Although references to material found on a Web site bear the date the material was accessed, the material available on the date cited may subsequently be removed from the site.

Non-NRC Reference Material

Documents available from public and special technical libraries include all open literature items, such as books, journal articles, and transactions, *Federal Register* notices, Federal and State legislation, and congressional reports. Such documents as theses, dissertations, foreign reports and translations, and non-NRC conference proceedings may be purchased from their sponsoring organization.

Copies of industry codes and standards used in a substantive manner in the NRC regulatory process are maintained at—

The NRC Technical Library
Two White Flint North
11545 Rockville Pike
Rockville, MD 20852–2738

These standards are available in the library for reference use by the public. Codes and standards are usually copyrighted and may be purchased from the originating organization or, if they are American National Standards, from—

American National Standards Institute
11 West 42nd Street
New York, NY 10036–8002
www.ansi.org
212–642–4900

Legally binding regulatory requirements are stated only in laws; NRC regulations; licenses, including technical specifications; or orders, not in NUREG-series publications. The views expressed in contractor-prepared publications in this series are not necessarily those of the NRC.

The NUREG series comprises (1) technical and administrative reports and books prepared by the staff (NUREG–XXXX) or agency contractors (NUREG/CR–XXXX), (2) proceedings of conferences (NUREG/CP–XXXX), (3) reports resulting from international agreements (NUREG/IA–XXXX), (4) brochures (NUREG/BR–XXXX), and (5) compilations of legal decisions and orders of the Commission and Atomic and Safety Licensing Boards and of Directors' decisions under Section 2.206 of NRC's regulations (NUREG–0750).

NUREG/IA-0401

International Agreement Report

Assessment of Two-Phase Critical Flow Models Performance in RELAP5 and TRACE Against Marviken Critical Flow Tests

Prepared by:
Lukasz Sokolowski
Tomasz Kozlowski

A. Calvo, NRC Project Manager

Office of Nuclear Regulatory Research
U.S. Nuclear Regulatory Commission
Washington, DC 20555-0001

Manuscript Completed: June 2011
Date Published: February 2012

Prepared as part of
The Agreement on Research Participation and Technical Exchange
Under the Thermal-Hydraulic Code Applications and Maintenance Program (CAMP)

Published by
U.S. Nuclear Regulatory Commission

Abstract

The project aims to (1) conduct the validation of thermal-hydraulics codes RELAP5 Mod 3.3 Patch 03 and TRACE v5.0 Patch 2 on the critical flow experiment giving comprehensive knowledge about the codes' behavior; (2) provide information about sensitivity impact of user-defined variables of critical two-phase models implemented into the codes; (3) and to obtain statistical data for variety of length-to-diameter L/D ratios of pipe. The experimental set-up consisted of vessel, discharge pipe and the group of test nozzles. The vessel was 24.5 m high, with internal average diameter of 5.2 m. The discharge pipe was 6.308 m long with internal diameter of 0.72 m. A total number of nine nozzles was used in the experiment and is characterized by L/D ratios of 0.3, 1.0, 1.5, 1.7, 3.0, 3.1, 3.6 and 3.7. The main conclusions of the studies are that for Marviken Critical Flow Test (CFT) (i) RELAP5 Henry-Fauske model gives more accurate results than RELAP5 Ransom-Trapp (R-T) model; (ii) TRACE R-T gives better results than RELAP5 R-T; and (iii) the dependence between length-to-diameter L/D ratio of the nozzle and the calculation's accuracy has not been observed.

Table of Contents

List of Figures

Executive Summary

The up-to-date thermal-hydraulics models and correlations are of the great importance in computational code environment. Thus, the validation of the systems codes is an important issue. The purpose of the project was to perform a comprehensive Marviken CFT investigation by a comparison between RELAP5 Mod 3.3 Patch 03 and TRACE v5.0 Patch 2 model data and experimental data. The main conclusions of the studies are that for Marviken CFT experiment:

• RELAP5 Henry-Fauske (RELAP H-F) model gives more accurate results than RELAP5 Ransom-Trapp (RELAP5 R-T) model;

• TRACE R-T gives better results than RELAP5 R-T;

• The dependence between length-to-diameter L/D ratio of the nozzle and the calculation's accuracy has not been observed.

Introduction

The aspects of safety are important in nuclear power plant maintenance and employ significant resources of engineer activity and wide varieties of tools. The thermal-hydraulics simulation codes play significant role in this work. They are basic tools for evaluation of safety aspects of nuclear reactors. It is crucial to ensure code's computational engine uses up-to-date correlations, definitions, and models. Thus, the RELAP5 Mod 3.3 Patch 03 and TRACE v5.0 Patch 2 validation on the Marviken Critical Flow Tests (CFT) experiment has been conducted.

The project aims to (1) conduct the validation of thermal-hydraulics codes RELAP5 and TRACE on the critical flow experiment giving comprehensive knowledge about the codes' behavior; (2) provide information about sensitivity impact of user-defined variables of critical two-phase models implemented into the codes; (3) and to obtain statistical data for variety of length-to-diameter L/D ratios of pipe.

The Marviken CFT experiment has been one of the biggest facilities in the world intended to test blowdown phenomena. It has been conducted in Sweden by an international project with participation from the Netherlands, Germany, France, USA, Denmark, Finland, Norway and Sweden. The experiment investigated the critical flow phenomena as a dependence on the discharge nozzle length-to-diameter ratio. The experimental set-up consisted of vessel, discharge pipe and the group of test nozzles. The vessel was 24.55 m high, with internal average diameter of 5.2 m. The discharge pipe was 6.3 m long with internal diameter of 0.72 m. The total number of nine nozzles was used in the experiment and is characterized by L/D ratios of 0.3, 1.0, 1.5, 1.7, 3.0, 3.1, 3.6 and 3.7.

The experiment was initiated when the pressure in the vessel was exceeding the rupture disc bursting pressure and the rupture disc was released. The bursting pressure was generally about 5 MPa but about 4 MPa for Test 5. The single test was finished when the steam reached the discharge pipe inlet or when the ball valve was closed. The data used to obtain a computational model, such as initial level of water, pressure, temperature, steam qualities, were obtained from the experimental data collected by measurement devices. Within the Marviken CFT experiment the total numbers of 27 experiments were conducted for different initial conditions and discharge nozzles.

As a part of a computational model development the following steps were undertaken. The components geometries were nodalized in order to match the RELAP5 and TRACE nodalization requirements with simplifying assumptions. The initial conditions were collected from the measurement data and implemented into the model input. Finally, the model's settings were adjusted.

The computational model provides the same information as the measurement data from the experiment. Moreover, the combination of models and assumptions can

be examined, e.g. comparison of critical flow models of Henry-Fauske and Ransom-Trapp. The sensitivity studies of these two models have been conducted.

The results have shown that the code's critical two-phase flow calculations' accuracy depends primarily on nodalization approximation and the type of a choking model. It can be stated that for Marviken CFT the Henry-Fauske model gives more accurate results compare to Ransom-Trapp model (both implemented in RELAP5 and TRACE) within the whole range of examined nozzles. The project results provide essential knowledge about the code behavior modeling blowdown phenomena, which is important in evaluation of the Loss of Coolant Accidents (LOCA).

The work was performed in the framework of power uprate project supported by the Swedish Radiation Safety Authority (SSM). The ultimate goal of this project is to perform independent analyses of some limiting transients associated to the power uprates. The present validation study is a Swedish contribution to the international Code Assessment and Maintenance Program (CAMP).

1. Two-Phase Critical Models

1.1. Critical Flow

The knowledge about the phenomenon of critical flow is important in evaluation of Loss of Coolant Accident (LOCA). Thus, it is important to know basic properties of a flow as a function of time, i.e. density, velocity of vapor and liquid, type of a flow.

The critical flow occurs when speed of flow equals speed of sound and is defined in terms of Mach number:

$$M = \frac{U}{c}, \tag{1.1}$$

where

U is the local speed of medium,

c is local speed of sound.

For different nature of the flow one will get:

- M > 1 supersonic flow,
- M = 1 critical flow,
- M < 1 subcritical flow.

The critical flow is also called as a choking flow. The fundamental reason that choking occurs is that acoustic signal can no longer propagate upstream. Simply put, the speed of sound is the maximum speed of the compressible fluid when it flows from the region of higher pressure to region of lower pressure.

The phenomenon of critical flow can be visualized in the following graphs. The discharge from the tank is presented where the p_o and p_R are the pressures inside the tank and at the end of the pipe, respectively.

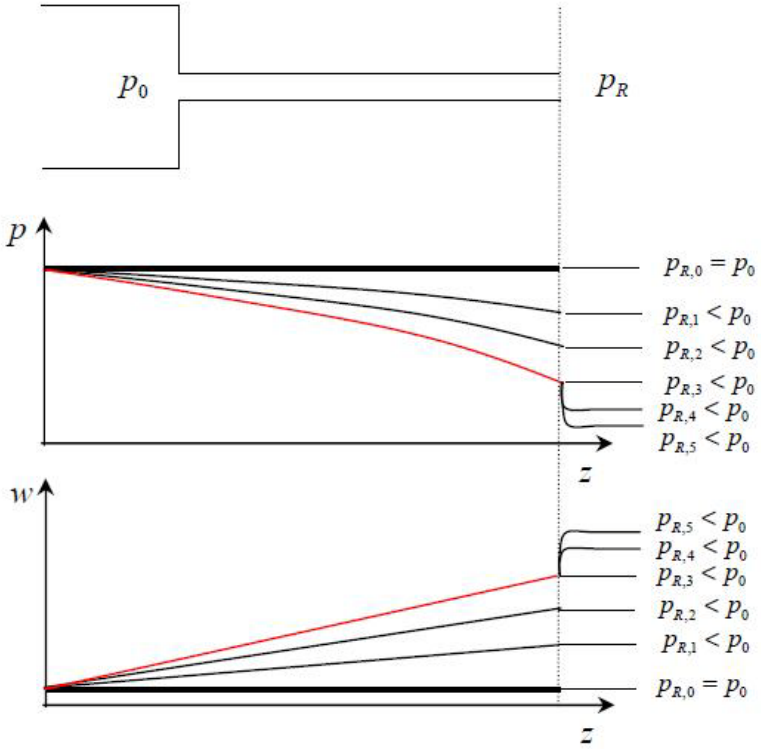

Figure 1.1 Critical pressure and mass flow velocity behaviors [1]

The critical mass flow rate depends only on stagnation parameters. As can be seen from the picture above, when downstream pressure p_R decreases the medium velocity *w* increases. However, the changes take place up to a point when the increasing in downstream pressure does not affect the process behavior. It can be seen in Fig. 1.1 that the downstream pressures $p_{R,3}$, $p_{R,4}$, and $p_{R,5}$ have identical impact on velocity of medium. This situation occurs since the choking occurs above pressure $p_{R,3}$.

The formula for single-phase critical mass flow rate can be derived from combination of the following equations [2]:

$$\frac{U^2}{2} + i = i_o \text{(energy equation)}, \tag{1.2}$$

$$i = \frac{\kappa}{\kappa - 1} RT = \frac{\kappa}{\kappa - 1} \frac{p}{\rho} \tag{1.3}$$

(gas enthalpy assuming isentropic transition),

$$\frac{\kappa}{\kappa-1}\frac{p}{\rho}RT=\frac{c^2}{\kappa-1} \text{ (assuming that } c=\sqrt{\kappa\frac{\partial p}{\partial \rho}}=\sqrt{\kappa\frac{p}{\rho}}=\sqrt{\kappa RT}\text{),} \tag{1.4}$$

where:

U – local velocity of medium,

i – downstream enthalpy,

i_o – stagnation enthalpy,

κ – Poisson's ratio,

p – pressure,

ρ – density,

R – gas constant,

T – temperature,

c – speed of sound.

In Eq. (1.2) symbol "0" refers to condition inside a tank or stagnation conditions. By combining Eqs. (1.2), (1.3) and (1.4) and assuming that the stagnation velocity is negligible and Mach number is 1 one will get:

$$c_* = c_0\sqrt{\frac{2}{\kappa+1}}\,. \tag{1.5}$$

The symbol of "*" refers to critical conditions. Assuming an isentropic process:

$$\frac{p^{\kappa-1}}{T^{\kappa}}=const\,, \tag{1.6}$$

$$\frac{T}{\rho^{\kappa-1}}=const \tag{1.7}$$

and employing ideal gas relations

$$\frac{p_*}{p_0}=\left(\frac{2}{\kappa+1}\right)^{\frac{\kappa}{\kappa-1}}, \tag{1.8}$$

$$\frac{\rho_*}{\rho_0} = \left(\frac{2}{\kappa+1}\right)^{\frac{1}{\kappa-1}}, \tag{1.9}$$

the critical flow rate will be as follows:

$$W_* = \rho_* U_* A_* = A_* \frac{p_0}{\sqrt{T_0}} \sqrt{\frac{\kappa}{R}} \sqrt{\left(\frac{2}{\kappa+1}\right)^{\frac{\kappa+1}{\kappa-1}}}, \tag{1.10}$$

where:

W – mass flow,

A – nozzle area,

T_o – stagnation temperature.

To state whether the single phase flow is at critical condition is an obvious task. To do the same with two-phase flow is much more complicated. The main reasons of that state are [1]:

- Two-phase (t-p) critical flow cannot be uniquely determined: there are two existing phases so that means there might be two speeds of sound – for liquid and for vapor,
- The complicated character of t-p flow, e.g. different flow regimes exhibited make the calculations complicated and time-consuming.

To overcome mentioned obstacles some modeling approximations need to be employed.

1.2. Two-Phase Critical Models

Starting from the 1947 (the first t-p critical model, proposed by J. G. Burnell) dozens of models describing critical t-p flow have been published. Critical flow models can be divided and classified with respect to:

- Model derivation technique,
- Model formulation,
- Undertaken assumptions,
- Output.

The first classification takes into account model's derivation:

- Theoretical background – employ thermodynamic equations of mass, momentum, and energy for both phase (liquid and vapor) separately or for homogeneous mixture,

- No theoretical background – semi-empirical formulas, linking critical flow rate to thermodynamic variables; dimensionless empirical coefficients adopted in order to fit the experimental data.

The last subcategory is of the interest for this project since the state-of-the-art in critical flow modeling is represented by models with no theoretical background as Henry-Fauske and Ransom-Trapp model. These two are the most widespread two-phase critical models.

To state that H-F and R-T do not have any theoretical background would be an oversimplification, see for instance the theory manuals of RELAP5 and TRACE, also paragraphs 1.3 and 1.4 below. So consider to reformulate.

The model formulation gives information about, e.g. number of conservation equation, i.e. of mass, momentum, energy, about number of state and/or transformation equations, constitutive equations, number of analytical conditions, and necessary semi-empirical parameters.

Undertaken assumptions provide information about transient phenomena, multidimensional-effect, non-homogeneity in pressure vessel, heat exchange with surrounding, pipes, orifices, etc.

Output subcategory is related to model applicability. Depends on parameters of interest, the different diagrams, thermodynamic variables, or correlations might be needed.

The main classification of two-phase critical flow models is presented in Fig. 1.2 (is this a novel figure or does it come from any reference, in the latter case please provide actual reference). The main divisions are models which assume thermodynamic equilibrium through the expansion line and models which assume non-thermodynamic equilibrium. The first mentioned category can be divided into homogeneous and non-homogeneous models. The non-equilibrium theory can be divided into “frozen” theories and non-homogeneous models.

“Frozen” models employ so called slip ratio. Slip ratio k provides information about the relative velocity between vapor and liquid. The k might have value of zero, constant, and non-constant through the expansion.

Homogeneous models assume that the liquid and vapor are mixed together and can be treated as a mixture. In this category there are Homogeneous Equilibrium Model (HEM) and Babitsky model. Non-homogeneous models assume that the vapor and liquid exist as separated phases. In this subcategory the value of k changes throughout the expansion line. Moody, Fauske and Levy models are given as examples.

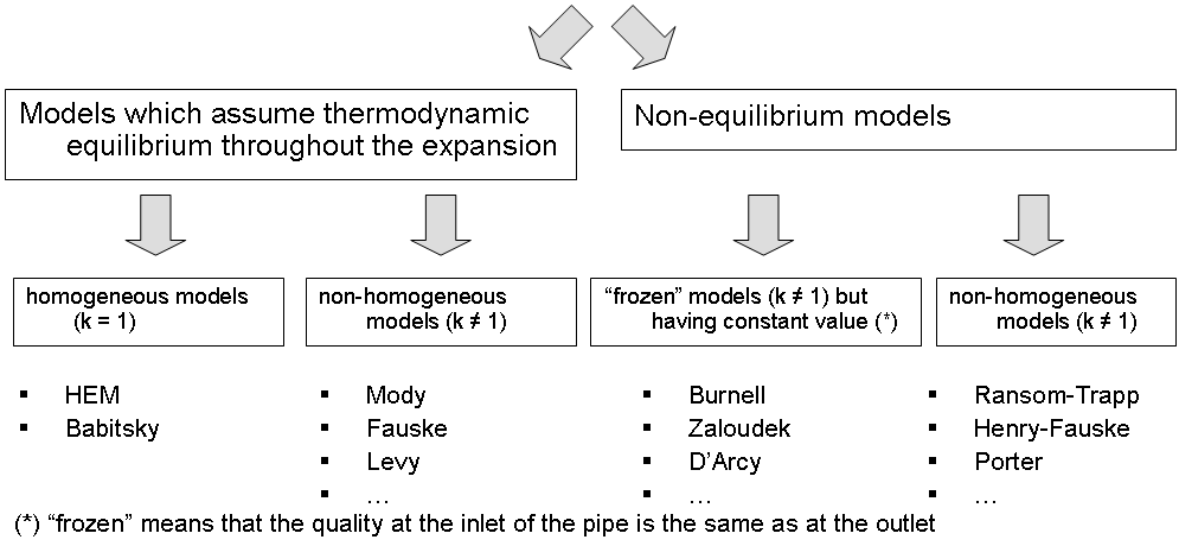

Figure 1.2 Classification of two-phase critical models

The non-equilibrium models assumed that between two-phases, vapor and liquid, there are no presence of:

- Thermal equilibrium,
- Dynamic (mechanical) equilibrium,
- Chemical equilibrium.

Thermal equilibrium means that both phases coexist at the same saturation conditions.

The dynamic equilibrium means that both phases are well-mixed, with equal velocity.

The chemical equilibrium means that both phases' densities do not change throughout the expansion.

The first category in non-equilibrium models are frozen theories with constant values *k*. Frozen means that there is no heat or mass transfer between the faces. Constant *k* denotes that there are no velocity changes through the expansion line. In this category there are models as e.g. Burnell, Zaloudek and D'Arcy.

The second subcategory of non-equilibrium models are non-homogeneous models with slip ratio different than 1. These models are the most complicated than all mentioned models. Within the last decades many models have been derived. However, the most important ones are the two models, Henry-Fauske and Ransom Trapp. It is worth to note that these two can be formulated as the simplest subcategory, in frozen models. The visualization of this classification is presented in the Fig. 1.3.

The first derivation of Henry-Fauske model is from 1970. This a non-homogeneous type that means there is no thermal, dynamic, or chemical equilibrium between phases. According to [4] this model type is suitable for length-to-diameter ratio L/D ≤ 3 to 12.

After developing this model, Henry and Fauske decided to release modified version of it. The frozen model was developed. The aim of the work was to provide ability of predicting two-phase critical flow sharing the knowledge only about the stagnation conditions and accounting for the non-equilibrium nature of the flow [4]. Another reason was that this model is simpler than full non-equilibrium one. The advantages of the simpler version is less calculations' time-consuming and computer storage. It is applicable only to long pipes, with L/D > 12.

The first Ransom-Trapp frozen model was released in 1978. The second version was the full non-equilibrium model published in 1982. The main goal of the work was to create a model having ability to predict critical flow rates with less sensitivity to the time step and the correct chocked flow velocity [5].

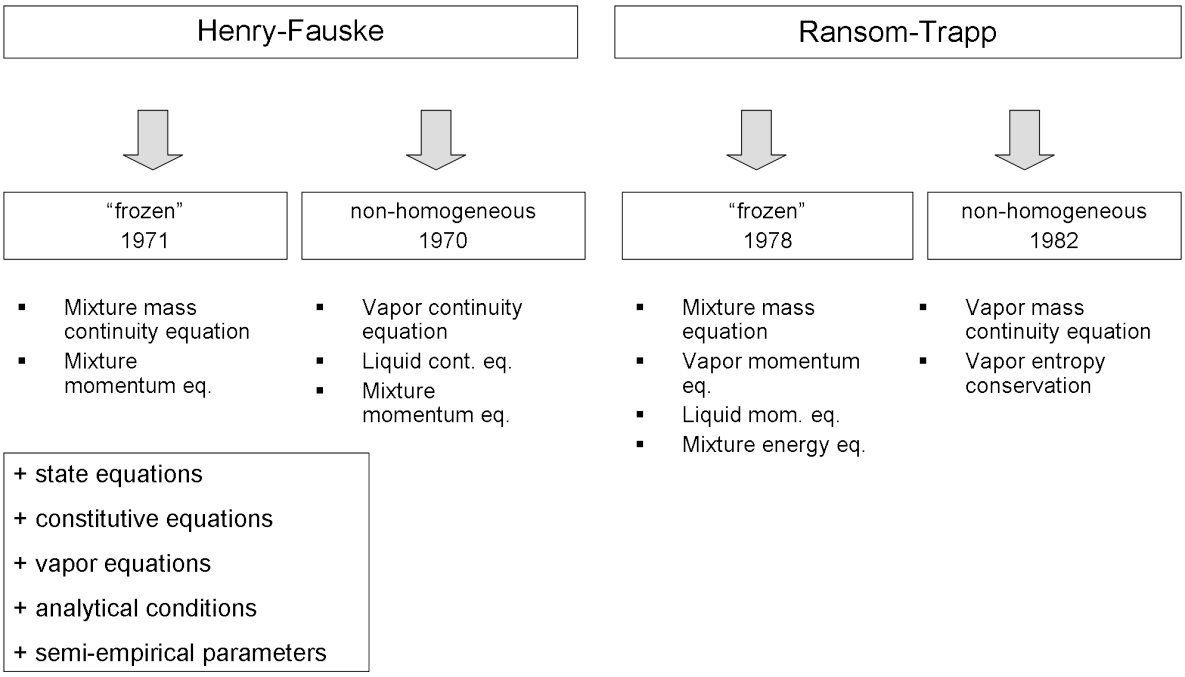

Figure 1.3 Henry-Fauske and Ransom-Trapp models' basic equations

The graph shows that to formulate the model, different equations and assumptions have been used.

1.3. Henry-Fauske Theoretical Background

By combination of one-dimensional momentum equation (1.11) and the mass flux for high velocities (1.12), [6],

$$-AdP = d\left(m_v u_v + m_l u_l\right) + dF\,, \tag{1.11}$$

$$G = -\left\{\frac{d\left[x u_v + (1-x)u_l\right]}{dP}\right\}_t, \tag{1.12}$$

the choking criterion will be obtained as

$$G_c^2 = \frac{-1}{\left\{x\frac{\partial v_v}{\partial P} + (1-x)\frac{\partial v_l}{\partial P} + \left(v_v - v_l\right)\frac{\partial x}{\partial P}\Big|_s\right\}_t} \tag{1.13}$$

where

G – mass flow rate,

x – quality,

v_v – vapor velocity,

v_l – liquid velocity,

P – pressure,

A – cross section,

$m_{v,l}$ – mass of vapor and liquid,

u – velocity of vapor and liquid,

F – wall shear stress.

Assuming that:

- Polytrophic expansion process affects the critical flow rate less than 1%,
- dv_g/dp determined from saturation properties (n ~ 1) [4],

equation (1.13) simplifies into

$$G_c^2 = \left(\frac{1}{\frac{N}{G_{cHE}} - v_g x_E \frac{dN}{dP}}\right)_e, \tag{1.14}$$

where G_{cHE} is the critical flow rate resulting from homogeneous equilibrium theory and N is a non-equilibrium parameter given by

$$N = \frac{v_f}{x_E(1-\alpha)v_g}, \tag{1.15}$$

where α is the void fraction.

As can be seen in Eq. (1.14), the total two-phase critical mass flow rate definition is based on equilibrium theory.

1.4. Ransom-Trapp Theoretical Background

Ransom-Trapp's two-fluid field under thermal equilibrium is described by the:

- Mixture continuity equation,

$$\frac{\partial \rho_m}{\partial t} + \frac{\partial}{\partial x}\left(\rho_m V\right) = 0, \tag{1.16}$$

- Two-phase momentum equations,

$$\alpha\rho_g\left[\frac{\partial V_g}{\partial t} + V_g\frac{\partial V_g}{\partial x}\right] + \alpha\frac{\partial \rho}{\partial x} + C\alpha(1-\alpha)\rho_m\left[\frac{\partial V_g}{\partial t} + V_l\frac{\partial V_g}{\partial x} - \frac{\partial V_l}{\partial t} - V_g\frac{\partial V}{\partial x}\right] = 0, \tag{1.17}$$

$$\begin{aligned}&(1-\alpha)\rho_l\left[\frac{\partial V}{\partial t} + V_l\frac{\partial V_l}{\partial x}\right] + (1-\alpha)\frac{\partial p}{\partial x}\\ &+ C\alpha(1-\alpha)\rho_m\left[\frac{\partial V_l}{\partial t} + V_g\frac{\partial V_l}{\partial x} - \frac{\partial V_g}{\partial t} - V_l\frac{\partial V_g}{\partial x}\right] = 0\end{aligned} \tag{1.18}$$

- Mixture energy equation,

$$\frac{\partial}{\partial t}\left(\rho_m s_m\right) + \frac{\partial}{\partial x}\left[\alpha\rho_g V_g s_g + (1-\alpha)\rho_l V_l s_l\right] = 0, \tag{1.19}$$

- Inert gas continuity equation,

$$\frac{\partial}{\partial t}\left(\alpha\rho_a\right) + \frac{\partial}{\partial x}\left(\alpha\rho_a V_g\right) = 0, \tag{1.20}$$

where:

ρ – density,

t – time,

V – velocity,

α – gas volume fraction,

C – virtual mass coefficient,

s – entropy;

subscripts:

m – mixture,

g – gas,

l – liquid,

α – noncondensable gas.

The Dalton's law is assumed (total pressure equals sum of partial pressures). The matrix representation of these equations is:

$$A\left(\overline{U}\right)\frac{\partial \overline{U}}{\partial t} + B\left(\overline{U}\right)\frac{\partial \overline{U}}{\partial x} = 0\,, \tag{1.21}$$

where $\overline{U}$ consists of p_v, α, V_g, V_l, and p_a. To solve the equation (1.21) the roots of the fifth-order polynomial needs to be obtained:

$$\text{determinant}\left(\underline{\underline{A}}\lambda - \underline{\underline{B}}\right) = 0\,. \tag{1.22}$$

Critical flow takes place if the maximum value of a characteristic root $\lambda_{i,re,max}$ is zero.

2. Marviken CFT Description

2.1. Historical Background

Marviken Critical Flow Tests experiment was conducted in 1978-1979 at the Marviken Power Station facility located around 100 km south-west of Stockholm.

It was supposed to be the fourth Swedish reactor and was called R4 or Eva. It was designed as a heavy water moderated reactor and intended to have power of 130 MW_e. However, due to technical and economic reasons it has been never used. The total cost of installation was 500 mln SEK. Today the installation works as an oil-fired power station.

It was decided that Marviken facility would be an experimental facility. Since 1972 to 1982 four series of experiment at Marviken facility was performed:

- Series I (green reports): The study of the pressure and temperature conditions during blowdown in pressure suppression containment. Following issues were investigated (16 experiments):
    - The effect of the energy content in the reactor and the steam in the reactor pressure vessel,
    - The location and size of the depth of vent pump submergence in the condensation pool,
- Series II (blue reports): The study of the dynamic process in the blowdown lines and the condensation pool (9 experiments),
- Series III (Critical Flow Test, yellow reports): The aim of this series was to determine the critical mass flow rate of a two-phase mixture of steam and hot water from large diameter pipe (27 experiments),
- Series IV (Jet Impingement Test, grey reports): The investigation of the effect of large-scale two-face phenomena in the containment (12 experiments).

The validation of RELAP5 code was performed based on Critical Flow Test (Series III). The Marviken Critical Flow Test (CFT) was conducted between January 1978 and May 1979. The experiment was performed by the international team from the Netherlands, Germany, France, USA, Denmark, Finland, Norway, and Sweden.

2.2. Description of the Test Facility

The facility consisted of several components which are [11]:

- The pressure vessel with net volume 425 m^3, maximum design pressure 5.75 MPa and maximum design temperature 272°C,

- The discharge pipe consisting of the ball valve and pipe spools which house the test nozzle upstream instrumentation,

- The nozzles and rupture disc assemblies: a set of nozzles of specified lengths and diameters to which the rupture disc assemblies were attached,

- The containment and exhaust pipes consisting of the drywell with net volume 1934 m^3, the wetwell with net volume 2144 m^3, the fuel element transport hall with net volume 303 m^3, the ground level 3.2 m diameter and the upper 0.4 m diameter exhaust pipe.

The outline of the facility is presented in Fig. 2.1.

In order to satisfy the experiment criteria some components inside the reactor vessel were removed while the other components were installed, e.g. measurement devices. Many components were removed from the vessel so that the flow rate was uninterrupted and the measurement of vessel net volume was simplified. However, some components were left but only if it was judged that they did not affect the experiment results significantly.

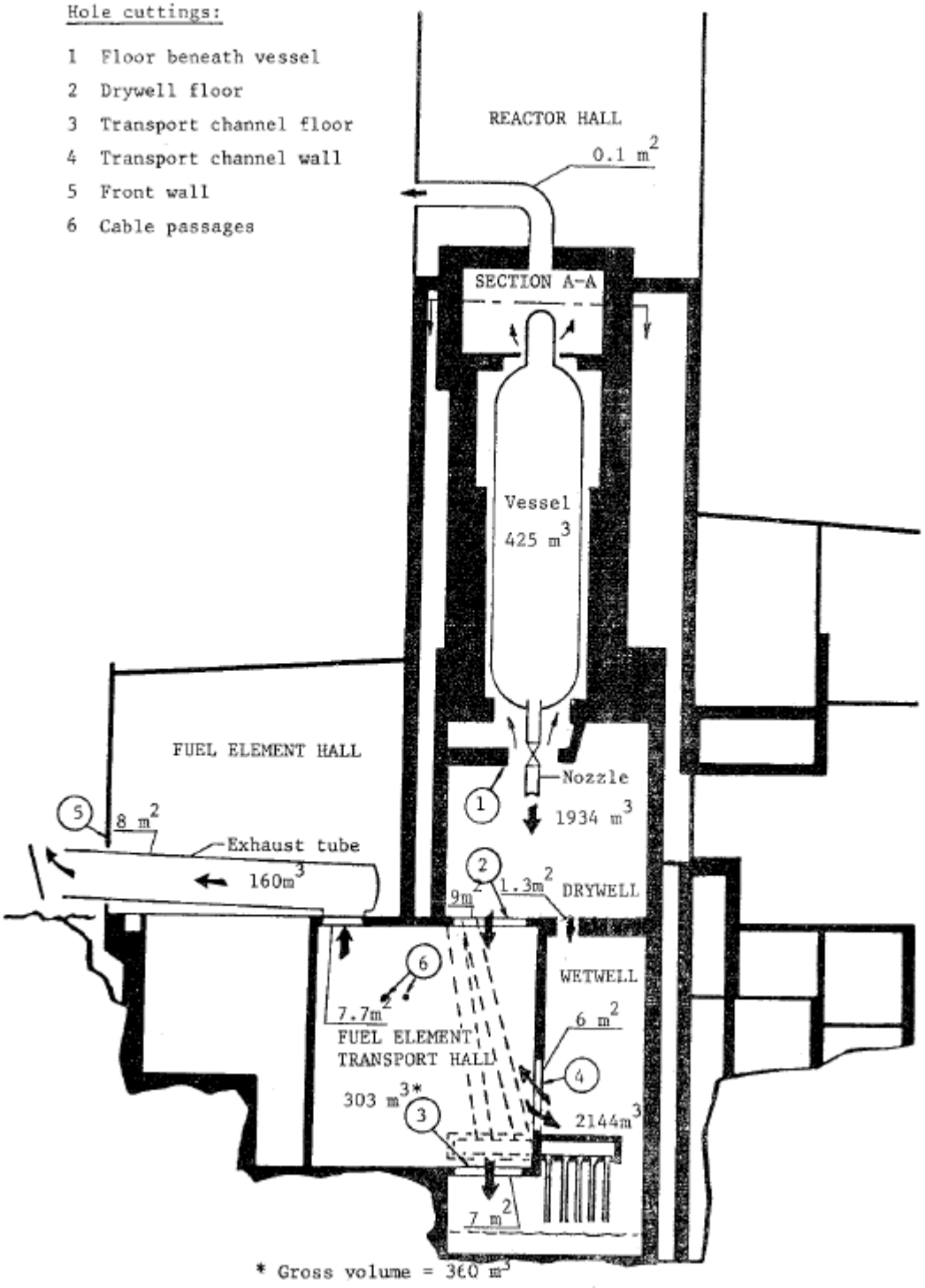

Figure 2.1 Outline diagram of the Marviken facility

2.2.1. Vessel

The pressure vessel was fastened and fully insulated using glass wool so that minimal heat transfer loss occurred. The vessel was of 24.55 m high and about 5.2 m inner diameter. The vessel was characterized by the elevation parameter which was 0 for the lowest point of the vessel and 24.55 m for the highest point. At the top of the vessel the cupola neck was located.

The vessel was made of low alloy steel, Swedish standard: DE-631A with a 76 mm wall thickness in the cylindrical part and a wall thickness of 40 and 65 mm in the domes.

Although most of the vessel internals were removed some components remained because of the difficulties in removing it. Some components were installed deliberately and had special function. Among these components are vortex mitigators, the primary pipes and instrumentation lines.

The vessel is visualized in the Fig. 2.2.

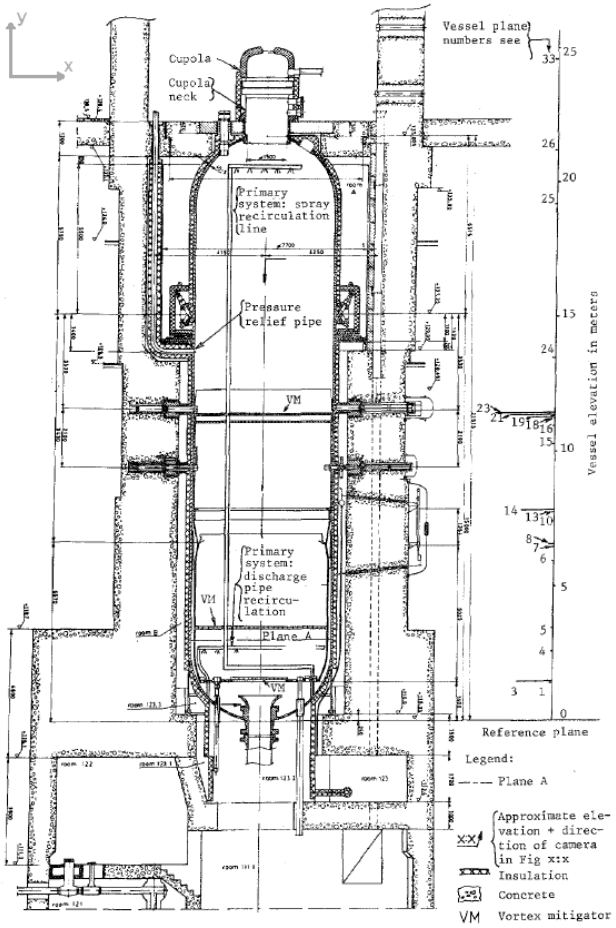

Figure 2.2 Vessel outline

2.2.2. Discharge Pipe

The discharge pipe connected the vessel and the nozzle. The total length of discharge pipe was 6308 mm including part in the vessel. The average inlet diameter was 752 mm. The discharge pipe can be seen in Fig. 2.3.

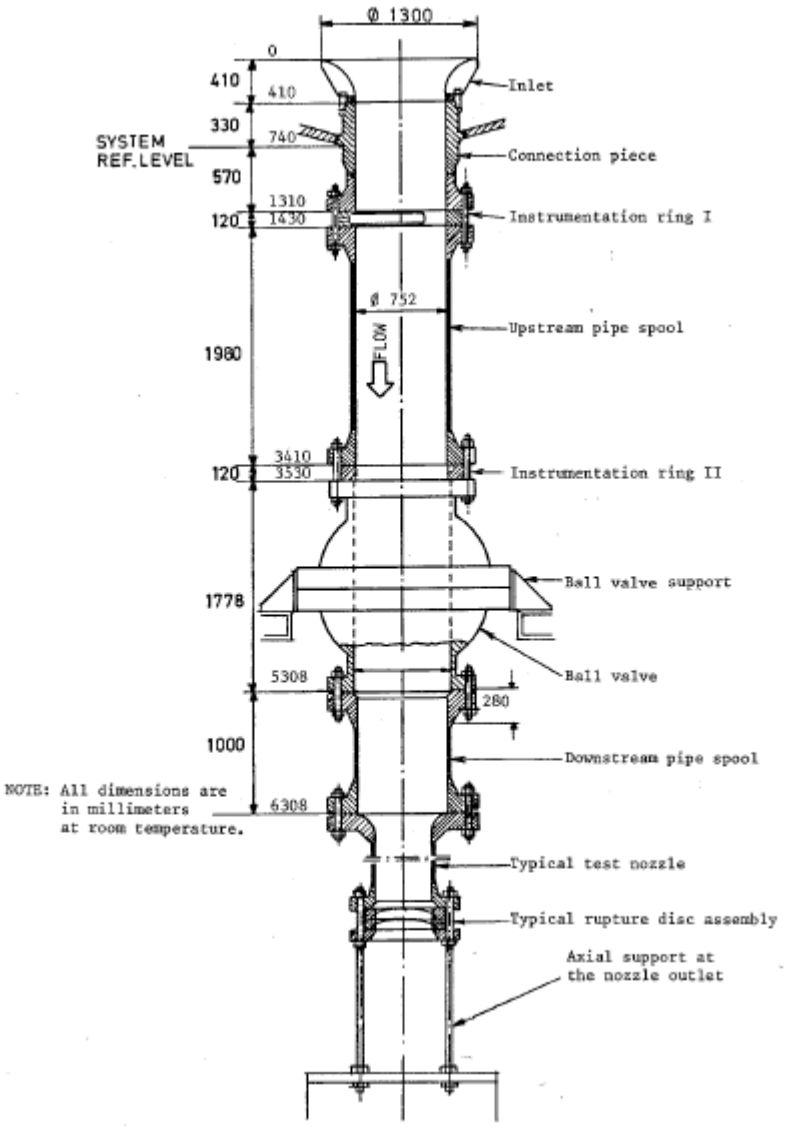

Figure 2.3 Discharge pipe

The discharge pipe was supported during the tests so that the oscillations did not exceed critical value. Inside the discharge pipe three instrumentation rings were placed. The measurement devices responsible for collecting information about pressure and temperature were located in the instrumentation ring.

The pipe was made of stainless steel, SIS 1330, Swedish Standard. The inlet had a wall thickness of 4 mm.

The ball valve was located in the discharge pipe. It could be closed within 10 seconds during the test.

2.2.3. Nozzles

The total numbers of nine nozzles were used in the experiment. Table 2.1 presents basic dimensions of the nozzles.

The nozzles' parameters and dimensions were chosen to provide full critical flow data in a wide spectrum of length-to-diameter ratio L/D. The maximum nozzle diameter was 509 mm and bigger diameter was not possible to test due to equipment constraint.

Table 2.1 Test nozzles – basic dimensions and conditions

Nozzle type no	D mm	L mm	L/D	L1 mm	L2 mm	L3 mm	L4 mm	R mm	Used in tests no
1	200	590	3,0	0	100	100	100	100	13, 14
2	300	290	1,0	55	150	150	150	150	6, 7
3	300	511	1.7	0	150	150	150	150	25, 26
4	300	895	3,0	55	150	150	150	150	1, 2, 12
5	300	1116	3.7	0	150	150	150	150	17, 18, 19
6	500	166	0.3	0	225	225	250	250	23, 24
7	500	730	1.5	0	225	225	250	250	20, 21, 22, 27
8	500	1809	3.6	0	181	156	241	250	15, 16
9	509	1589	3.1	55	156	225	241	250	3, 4, 5, 8, 9, 10, 11

For the first 12 tests the nozzle with flared outlet were used, as shown in Fig. 2.4. Later it was decided to that the nozzles should have constant diameter test section which would exhaust a free expansion jet into the containment [12].

Nozzle used for test 13 and 14 is presented in Fig. 2.5. Nozzle geometry used for tests 15 onwards is visualized in Fig. 2.6.

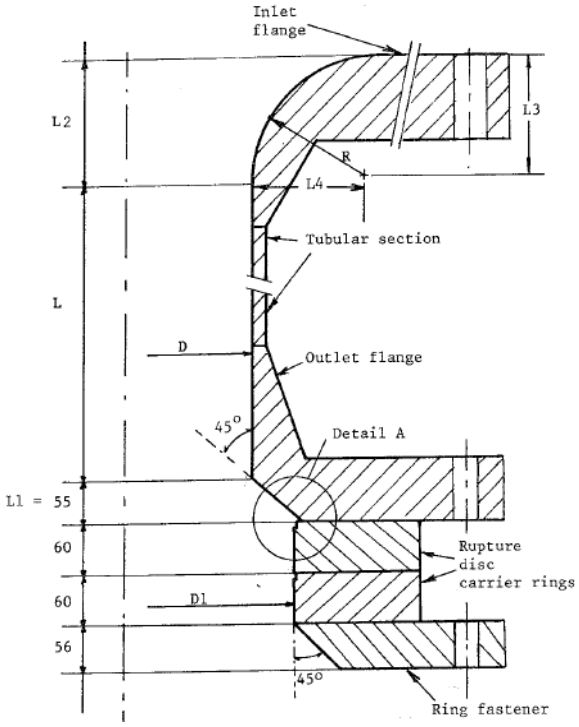

Figure 2.4 Dimensions of the test nozzle used for tests 1-12 [12]

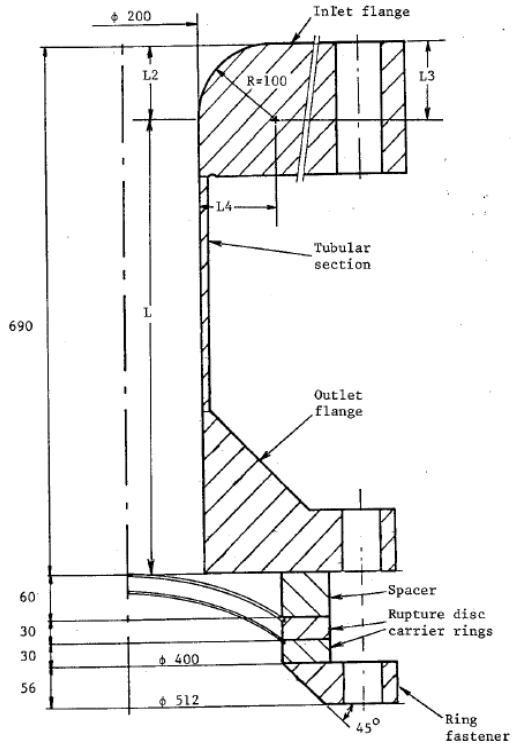

Figure 2.5 Dimensions of the test nozzle used for tests 13-14 [12]

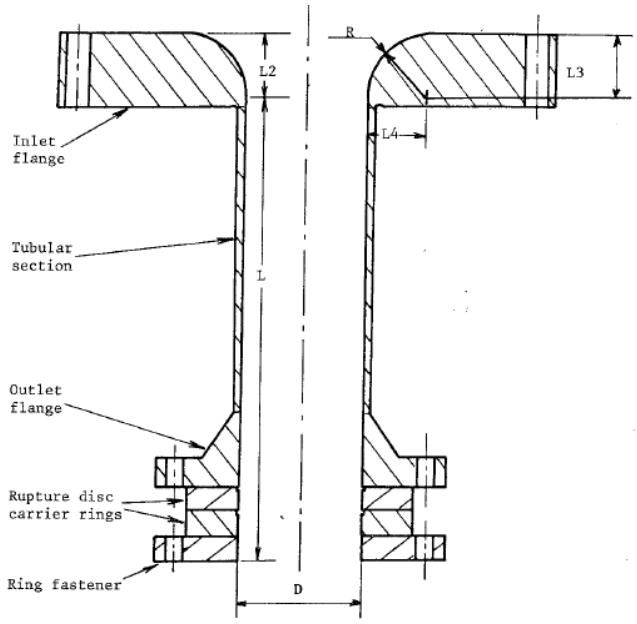

Figure 2.6 Dimensions of the test nozzle used for tests 15-27 [12]

2.3. Experiment

Within the Marviken CFT the total number of 27 tests was performed during which the nozzles with different length-to-diameter L/D ratio were examining. Tests were conducted under different conditions in the vessel. Appendix A presents summary of initial and final conditions in the vessel.

The average pressure in the vessel was about 5 MPa, only Test 5 was performed at 4 MPa. The water level varied from 16.5 to about 20 m.

The test period varied from 42 sec for Test 3 and to around 148 sec for Test 13.The test was finished when the steam reached the discharge pipe or the ball valve was closed.

2.4. Measurement System

Fig. 2.7 and 2.8 show locations of measurement devices used during the experiment.

For the modeling purposes, the vessel, data channel number of 101 and 104 were for pressure measurement, and 401, 402, 501 to 520 were used for temperature measurement.

In the discharge pipe, data channel numbers from 107 to 109 were used for pressure measurement and 31, 37 to 39 for temperature measurement.

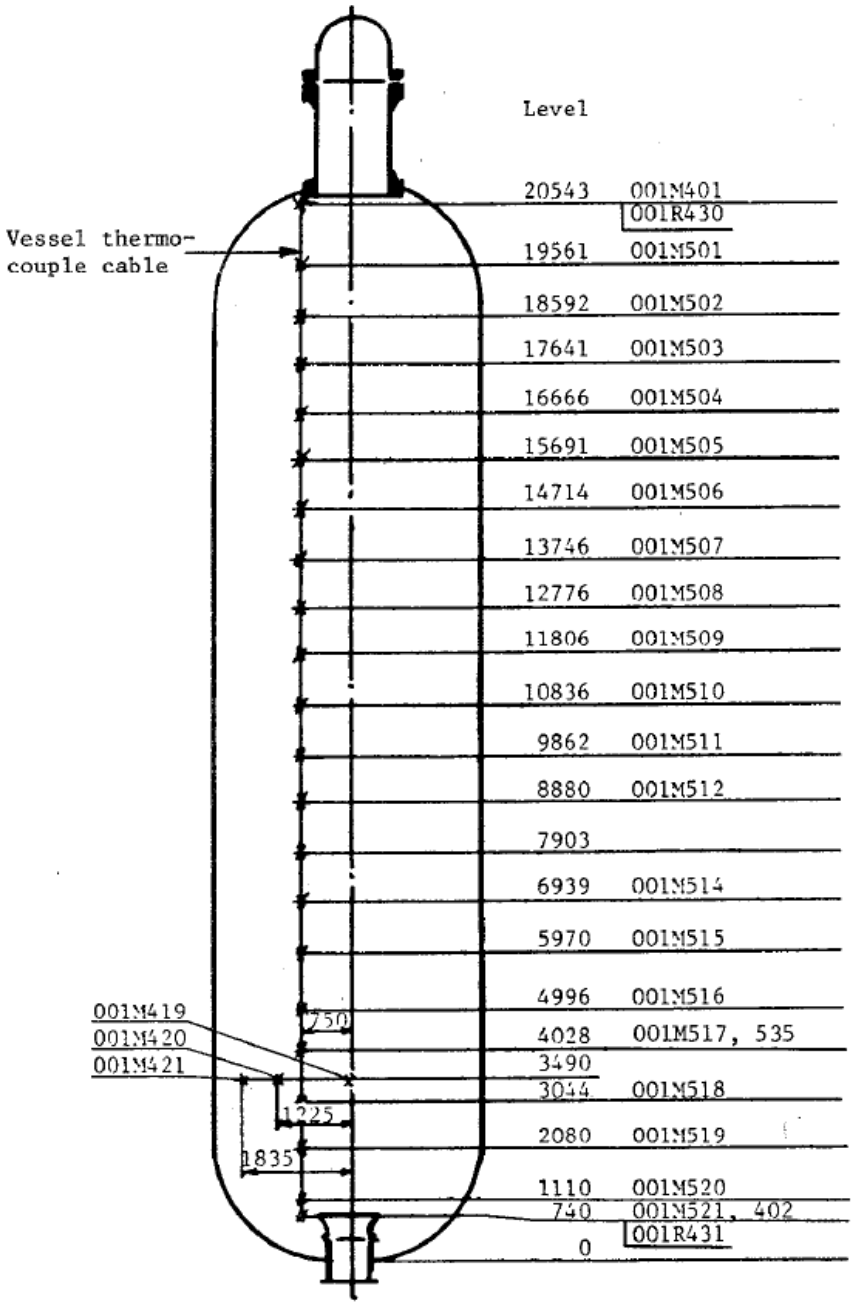

Figure 2.7 Locations of temperature measurements in the pressure vessel [11]

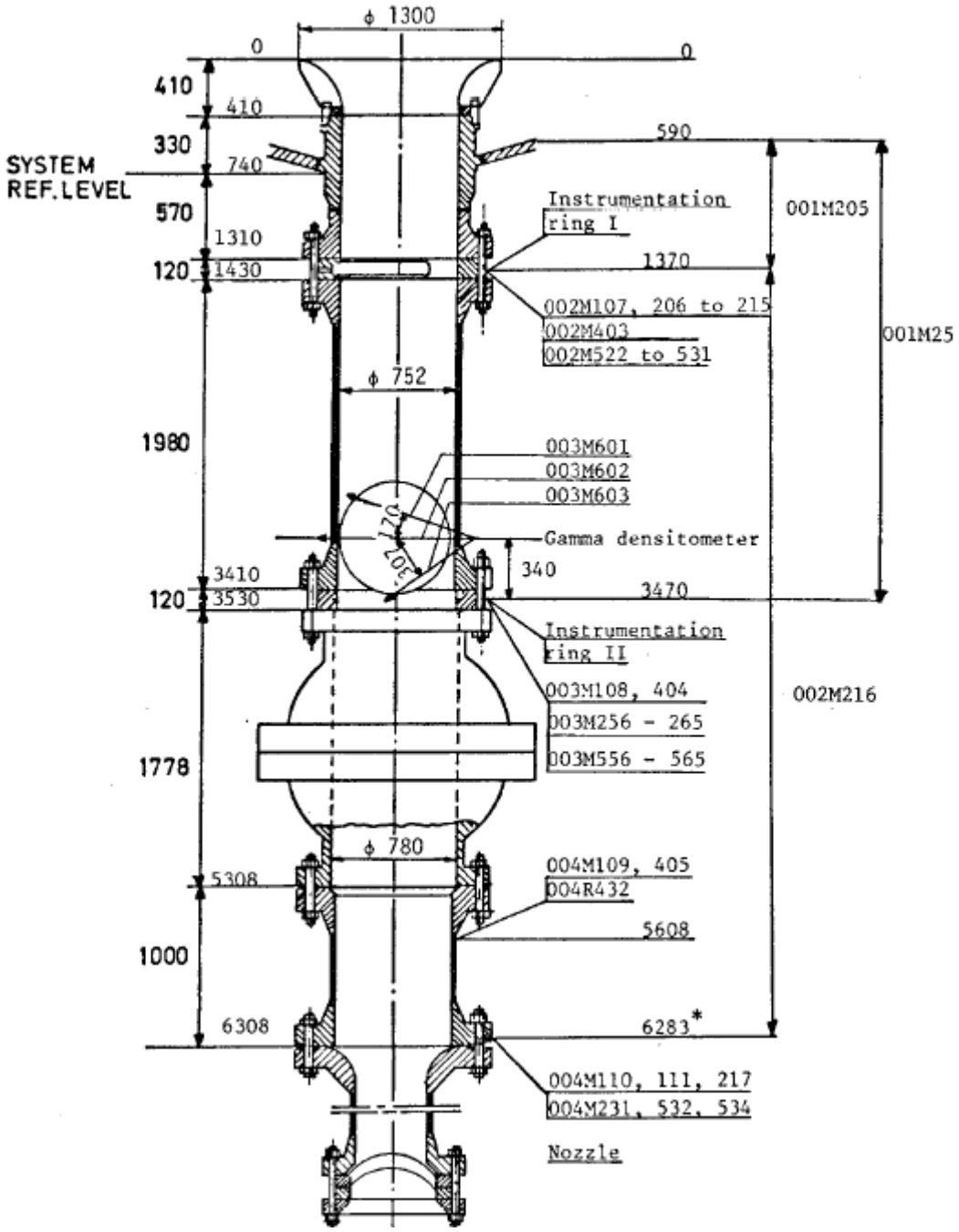

Figure 2.8 Locations of measurements in the discharge pipe [15]

3. Modeling & Simulation

3.1. Modeling Approach

Modeling of Marviken CFT experiment was conducted in the following steps: nodalization, adjusting the initial conditions and formulating the code input files.

The RELAP5 Mod 3.3 Patch 03 and TRACE v.50 Patch2 computational model was created based on the Marviken facility description [11], [12], [16]. The model nodalization was adjusted to satisfy the condition that the calculation should not be time-consuming and should be possibility to run the calculations on commonly available personal computers. The guides provided by the code's developer were followed [9], [20], [21].

The default values (1.0) of choking model input parameters were used for all choking models: subcooled, two-phase, and superheated discharge coefficients for R-T and discharge coefficient and thermal nonequilibrium constant for H-F, are treated as important model characteristics.

3.2. Nodalization

The RELAP5 computational model was created based on the Marviken facility description. TRACE model was based on the RELAP5 model to make both models consistent with each other. The RELAP5 computational model consisted of two pipe components, two single junctions, and time dependent volume. The TRACE computational model consisted of two pipe components and a brake. The first pipe component modeled the vessel. It consisted of 21 volumes. The first two volumes simulate the cupola, cupola neck, and the vessel top. The next 18 volumes are the same and have the length of 967 mm and diameter of 5.2 m. The last volume is simulates the vessel bottom.

The second pipe component was a model of discharge pipe and nozzle. This component consisted of 15 volumes. The first 13 volumes correspond to the discharge pipe and the last 2 volumes correspond to the nozzle. The discharge pipe and nozzle nodalization was constant for all simulations. The nodalization of the computational model is shown in Fig. 3.1.

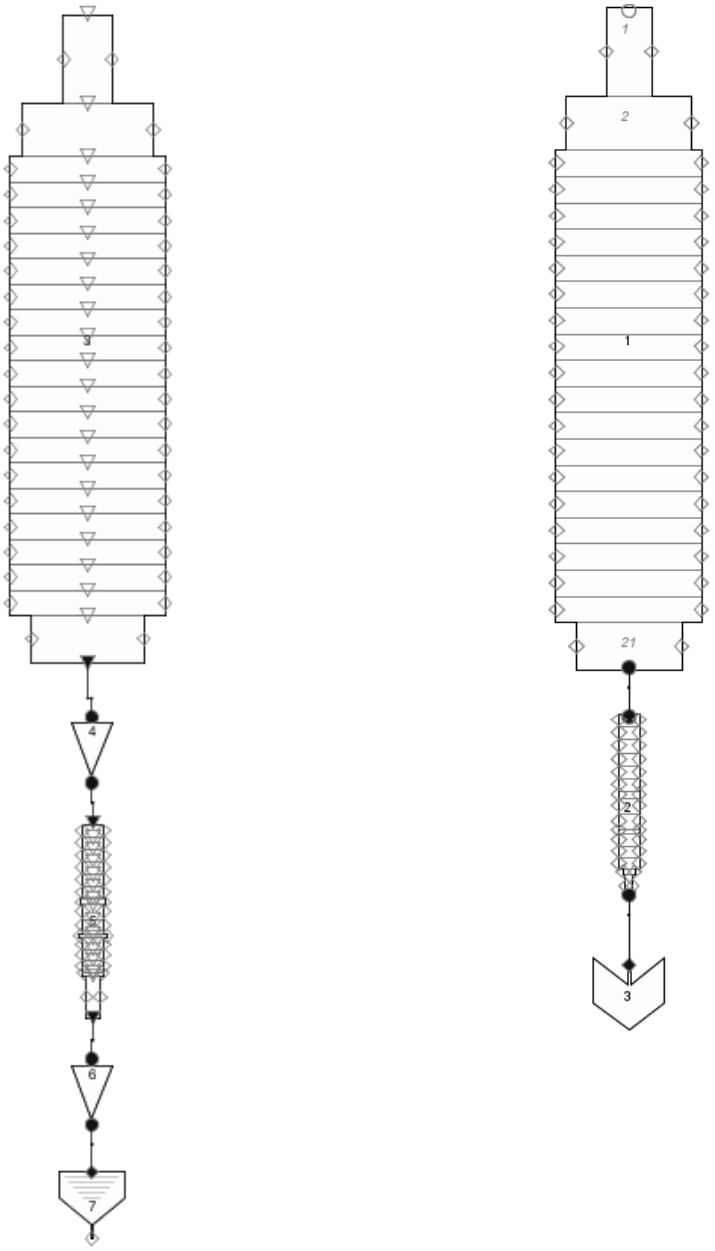

Figure 3.1 Visualization of the final nodalization used in the calculations; RELAP5 (left) and TRACE (right)

The RELAP5 time dependent volume and TRACE break component is 1 m long and the flow area was equal to the area of the nozzle.

The nodalization process is a complex task in which user experience is very essential. The example approaches that were tested are shown in Fig. 3.2.

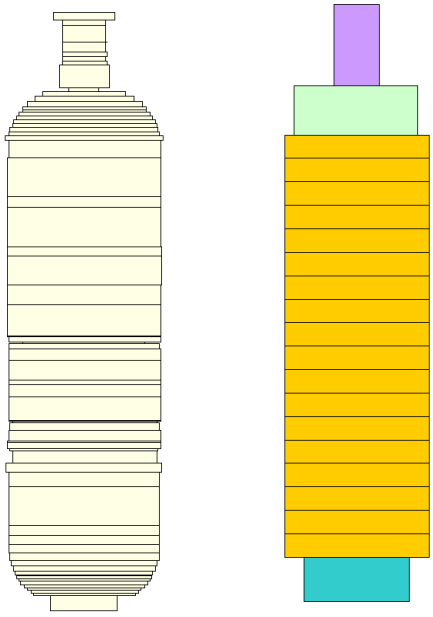

Figure 3.2 Nodalization approaches: fine model (left) and coarse model (right)

The first nodalization was an ideal geometry taken from the Marviken facility description [12]. It was divided into six zones, which were then subjected to simplification. During this process the length and the volume of the vessel was conserved. The final nodalization is the final one which was used for calculations.

The number of cells can be reduced without significantly changing the performance of the model and simulation. The advantage is that the calculation time is much lower for models with smaller cell number. However, it should be kept in mind that sometimes when the number of cells is too low, the model's accuracy becomes unacceptable. The example of the fine and coarse model performance is shown in Fig. 3.3.

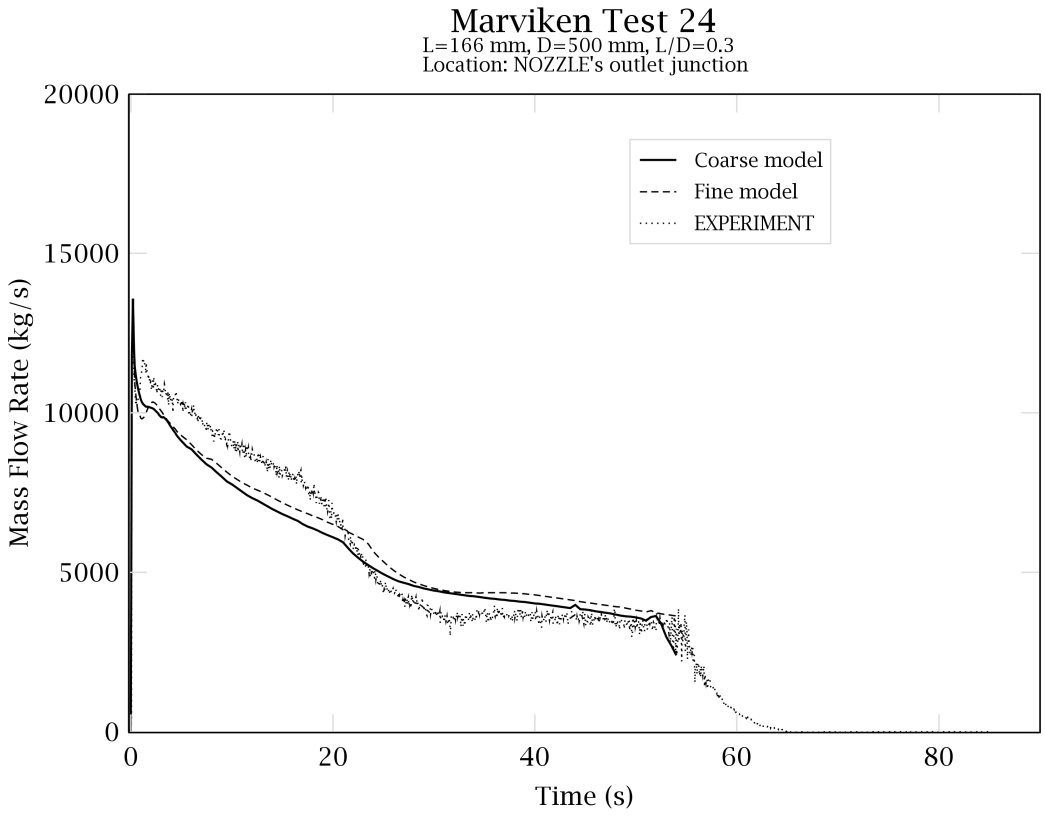

Figure 3.3 Comparison of the different approaches' performance

Fine course model gives quantitatively the same result, therefore course model was deemed acceptable.

The discharge pipe nozzle component consists of 15 cells. The two last cells are intended to simulate the nozzle. The discharge pipe was the same for the all experiments. The full abrupt area change model was applied on junction no. 7 and 10 in discharge pipe, to take into account the abrupt in the location of instrumentation ring II and abrupt in the location of ball valve, respectively. No further nodalization studies were done for the discharge pipe.

The visualization of the discharge pipe and nozzle components nodalization is shown in Fig. 3.4.

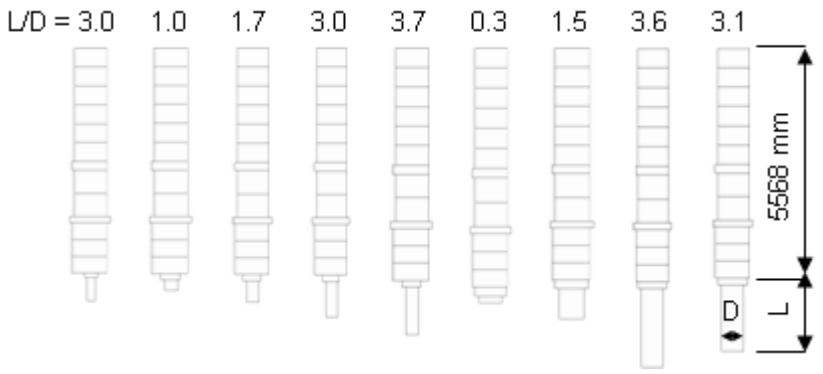

Figure 3.4 Nodalization of nozzles used in the computational model

3.3. Initial Conditions

Data necessary to determine initial conditions in the model was obtained from measurement. Appendix B presents data channels used in the computational model initial conditions.

The negative value of elevation level denotes that the measurement device was located in the discharge pipe.

As can be seen in the Appendix A, the different initial conditions were used for each experiment. The saturated zone, transition zone and subcooled zone in the vessel can be identified.

Fig. 3.5 shows vessel zones denotation and arrangement.

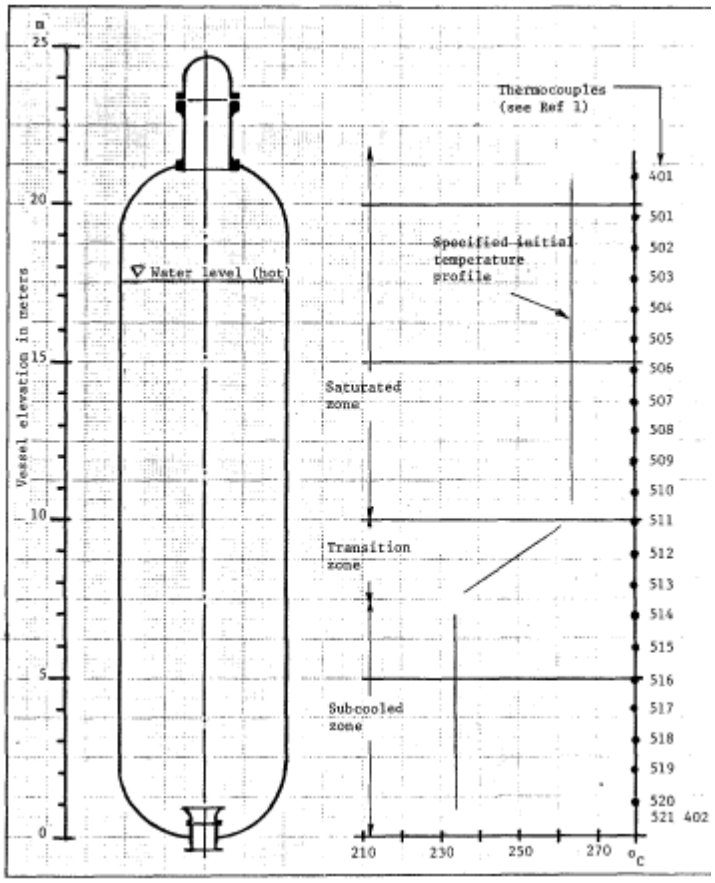

Figure 3.5 Vessel zones denotation and arrangement

The shape and the range of different zones were different for each experiment. Thus, the experiments were categorized in three categories depend on the type of initial conditions in the vessel.

Initial conditions category I test denotes that the test was conducted with water initially subcooled 15 °C or more.

Initial condition category II test denotes that the test was conducted with water initially subcooled 30 °C or more.

Initial condition category III test denotes that the test was conducted with water initially subcooled less than 5 °C. Fig. 3.6 shows the test matrix for sample tests.

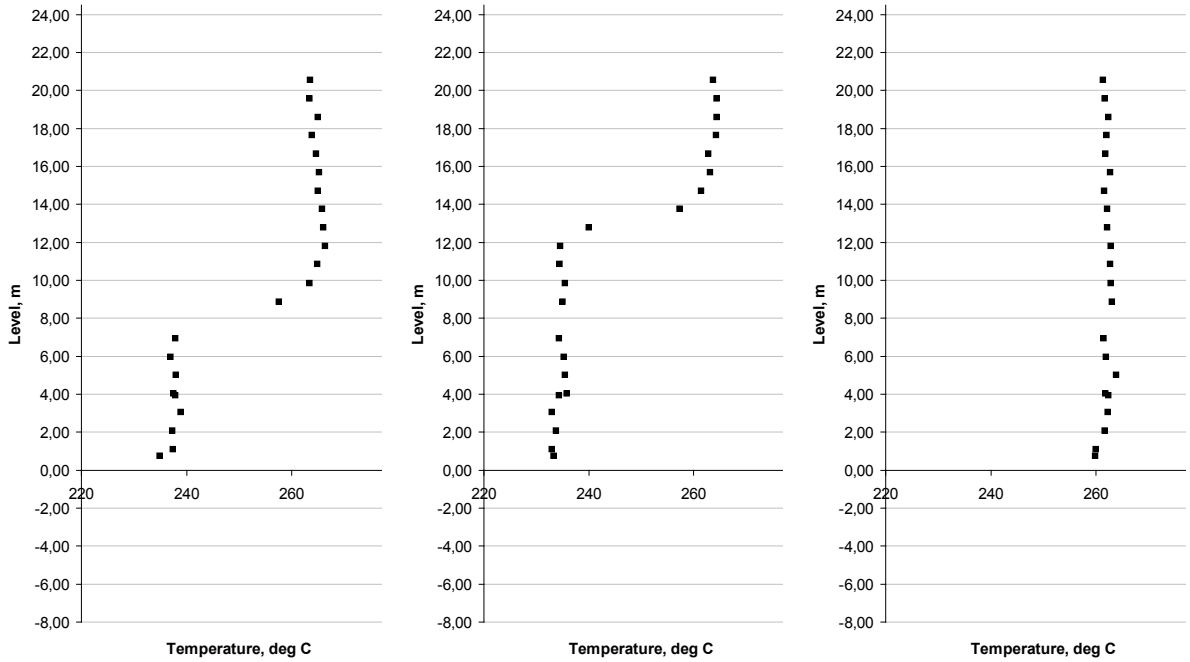

Figure 3.6 Vessel matrixes (from left: Category I Marviken Test 13, Category II Marviken Test 15, Category III Marviken 14)

For statistical purposes it is worth to connect initial condition category with different nozzle types what is shown in Table 3.1.

Table 3.1 Vessel categories and nozzle types

Initial condition category type	Test no $^{\text{Nozzle no}}$
I	1^4, 2^4, 3^9, 4^9, 5^9, 6^2, 7^2, 8^9, 11^9, 12^4, 13^1, 16^8, 18^5
II	15^8, 17^5, 21^7, 22^7, 24^6, 26^3, 27^7, 22^7
III	9^9, 10^9, 14^1, 19^5, 20^7, 23^6, 25^3

3.4. Numerical Solution Accuracy Quantification

Quantification of systems code accuracy is important in the validation process.

The L1 and L2 norm method have been employed in this work:

$$L_{1,rel} = \frac{1}{N}\sum_{i=1}^{N}\left|\frac{c_i - e_i}{e_i}\right|, \tag{4.1}$$

$$L_{2,rel} = \sqrt{\frac{1}{N}\sum_{i=1}^{N}\left(\frac{c_i - e_i}{e_i}\right)^2}\ , \tag{4.2}$$

where:

$L_{1,rel}$ – L1 norm, relative,

$L_{2,rel}$ – L2 norm, relative,

N – number of data points,

c – calculated data,

e – experimental data,

and standard deviation:

$$\sigma = \sqrt{\frac{1}{N}\sum_{i=1}^{N}\left(e_i - \bar{e}\right)^2}\ , \tag{4.3}$$

where

σ – standard deviation,

$\bar{e}$ – mean value of N data.

4. Validation and Results

4.1. Background

The results from the comparison between two-phase critical models of Henry-Fauske and Ransom-Trapp are presented in this Chapter. In the next subsections the sensitivity studies of the computational model are presented.

It is not intended to present the predicted flow rate results from every single experiment in this Chapter. These can be found in Appendix C. However, some selected results will be presented in order to show essential information about the code's behavior, simulation technique or particular solution feature.

4.2. Sensitivity Studies

The models sensitivity was investigated. The magnitude of influence of parameters having significant contribution to the simulation results were determined by examining following parameters.

4.2.1. Initial Conditions (RELAP5)

Fig. 3.6 in Chapter 3 shows three types of initial conditions in the vessel. The descriptions of each single vessel zones were provided in the mentioned Chapter.

In the RELAP5 model the saturated and transition zone was described by pressure-quality [p,x] initial condition type. The subcooled zone was described by pressure-temperature [p,T] initial condition type.

However, for category III initial condition tests and for some tests from category II, it was hard to determine single zone. Thus, it was decided that in such a situation the initial conditions in the vessel were described by [p,x] conditions. This is because for this type of condition it is easier to determine whether the medium is liquid [x = 1] or vapor [x = 0]. For [p,T] initial condition such a determination is more difficult since it depends on RELAP5 water properties tables.

Distinctions in usage of different initial condition types are shown in Fig. 4.1.

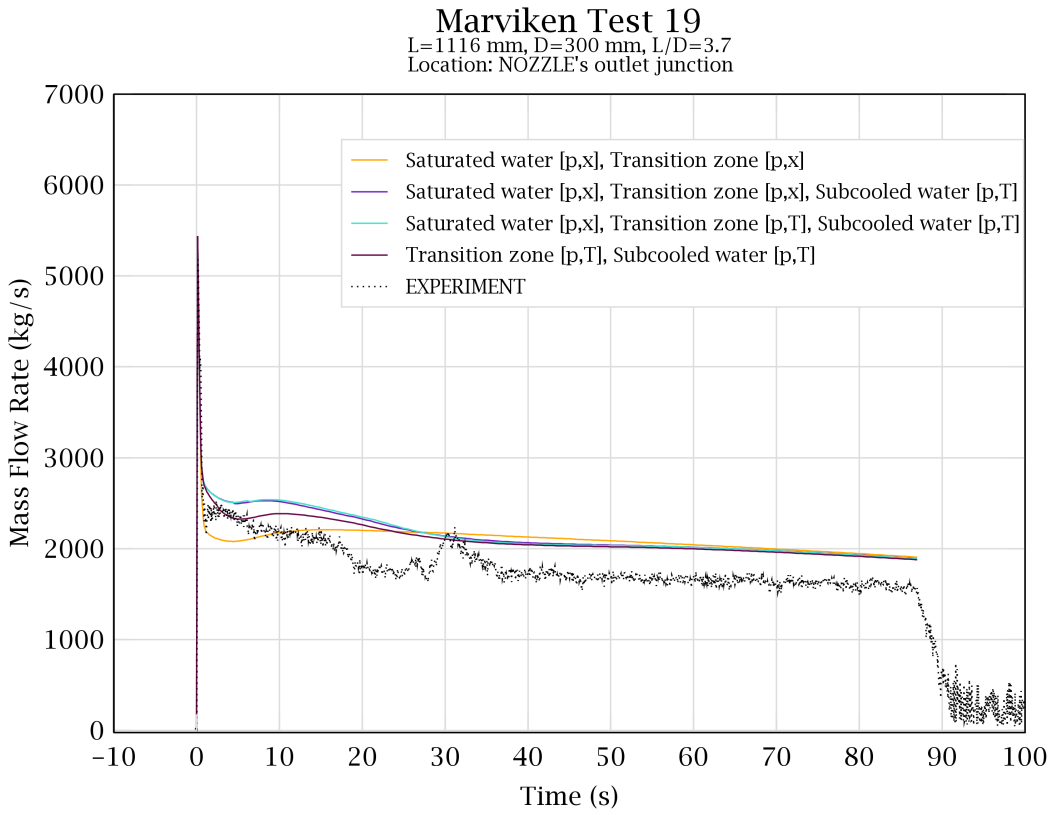

Figure 4.1 Distinctions in usage of different initial condition types

The essential difference in results can be observed between the case when all vessel zones were determined by [p,x] condition and condition were the transition zone is determined by [p,T].

If the water is at saturation state it is recommended to use [p,x] initial condition type instead of [p,T] initial condition type.

4.2.2. Discharge Pipe Length

For the modeling purposes it was assumed that the discharge pipe length is 5568 mm. The 740 mm of the discharge pipe inside the vessel was neglected. However, the investigation whether such an approach influence much the simulation was conducted.

Fig 4.2 shows different approaches of the discharge pipe modeling.

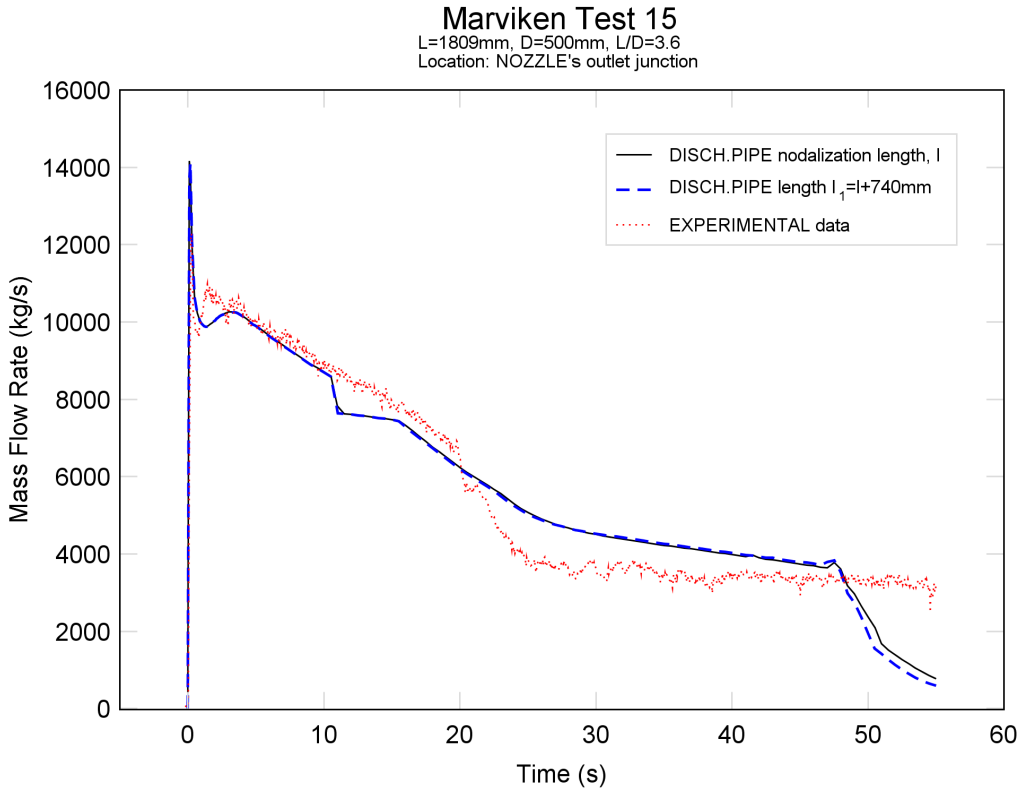

Figure 4.2 Different approaches of the discharge pipe modeling

As can be seen from the figure the differences between the two approaches are negligible thus it is recommended to use the simplified geometry of the discharge pipe.

4.2.3. Junction Control Flag

Junction control flags are next to nodalization, one of the most important parameters in RELAP5 modeling.

In the computational the models of abrupt and chocking were in use:

- choking option specifies, whether (1) choking model is applied or (2) choking model is not applied,
- abrupt option specifies whether (1) the smooth option is applied, or (2) abrupt option is applied but without code's calculations of forward and reverse coefficient K_{loss}, or (3) abrupt option is not applied.

Some tests were characterized by occurrence of characteristics dip after above 10 seconds, as shown in Fig. 4.3. This phenomenon occurs in simulation because chocking flow is predicted in the last 2 junctions. Such a behavior can be avoided by applying the choking model only at the last junction.

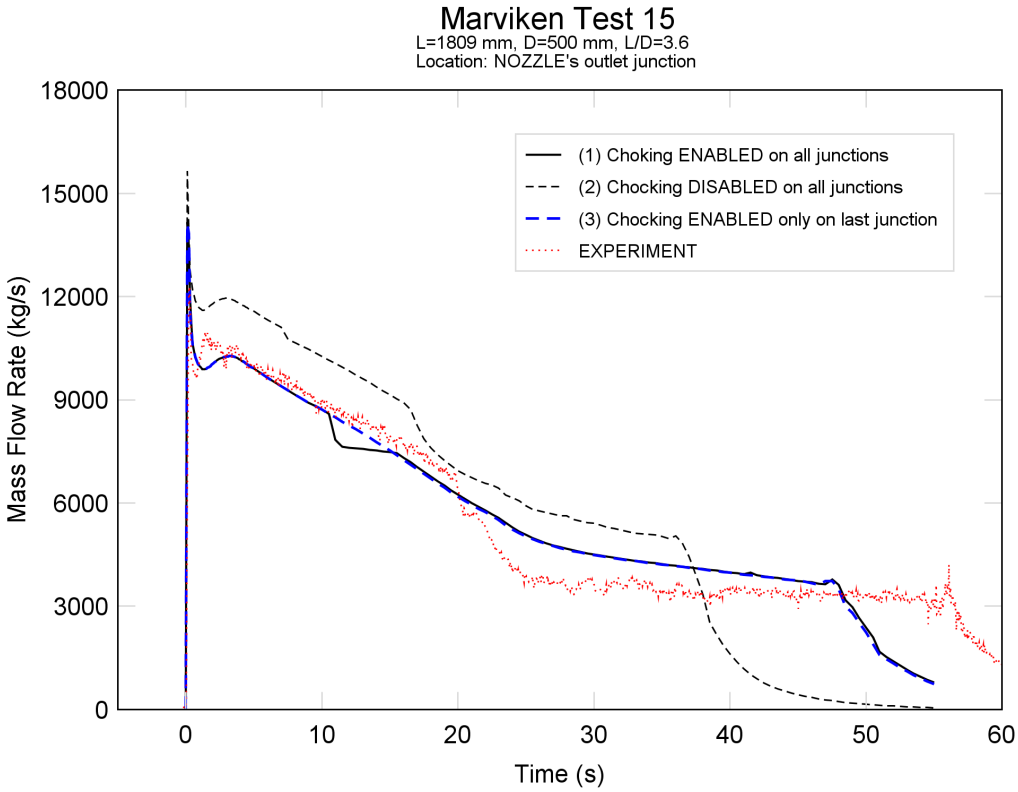

Figure 4.3 Different choking options

4.2.4. Loss Coefficient

Loss coefficient is important parameter in thermal-hydraulics calculations. It provides information about the pressure losses. Although the information about the loss coefficient was not provided in the facility description, the sensitivity studies with using forward loss coefficient model were performed.

For forward loss coefficient K = 0.04 the calculations was performed for Test 24, the smallest length-to-diameter L/D ratio experiment. Such a loss coefficient does not affect appreciably the mass flow rate.

4.2.5. Time Dependent Volume (RELAP5)

Time dependent volume is the component which is used as an outlet pressure boundary condition. The sensitivity calculations were conducted using following parameters:

- Case 1: A = 0.1964 m^2, L = 1.0 m,
- Case 2: A = 0.1964 m^2, L = 0.5 m,
- Case 3: A = 0.400 m^2, L = 1.0 m.

The area for case 1 and 2 is equal to nozzle area for Test 24.

It was observed that the length of an area the time dependent volume do not affect appreciably the mass flow rate.

4.3. Henry-Fauske and Ransom-Trapp Performance

The performance of two-phase critical models, Henry-Fauske (RELAP5) and Ransom-Trapp (RELAP5 and TRACE), is presented in this subsection.

The first part shows the plots where the measured vs. calculated data are shown. This is necessary to determine whether code tends to under or over-predict. The straight line shows the perfect code prediction. The left bottom part of the plot is the region where the test ends. The right upper part of the plot is the region where the test starts. The data from all Marviken experiment (except Test no. 10: no available data) have been shown to these plots.

The second subsection is focused on models' performance with respect to the length-to-diameter ratio (L/D).

4.3.1. Code Accuracy

The convenient but approximate way to compare measured and calculated data is to plot these two in the same graph. In this subsection such a comparison was done for two models implemented in RELAP5 and one model in TRACE.

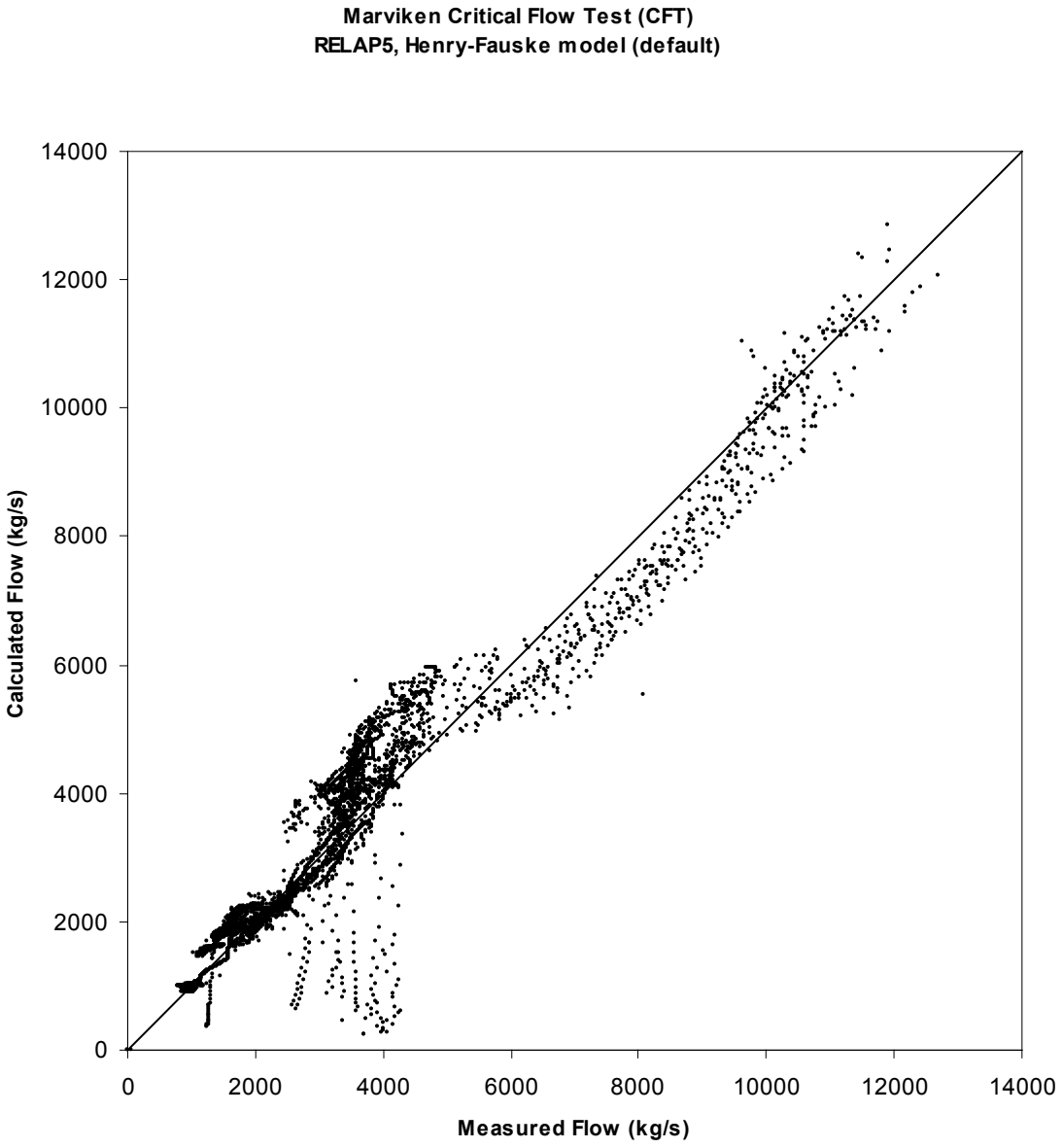

Figure 4.4 Code accuracy, RELAP5 Henry-Fauske

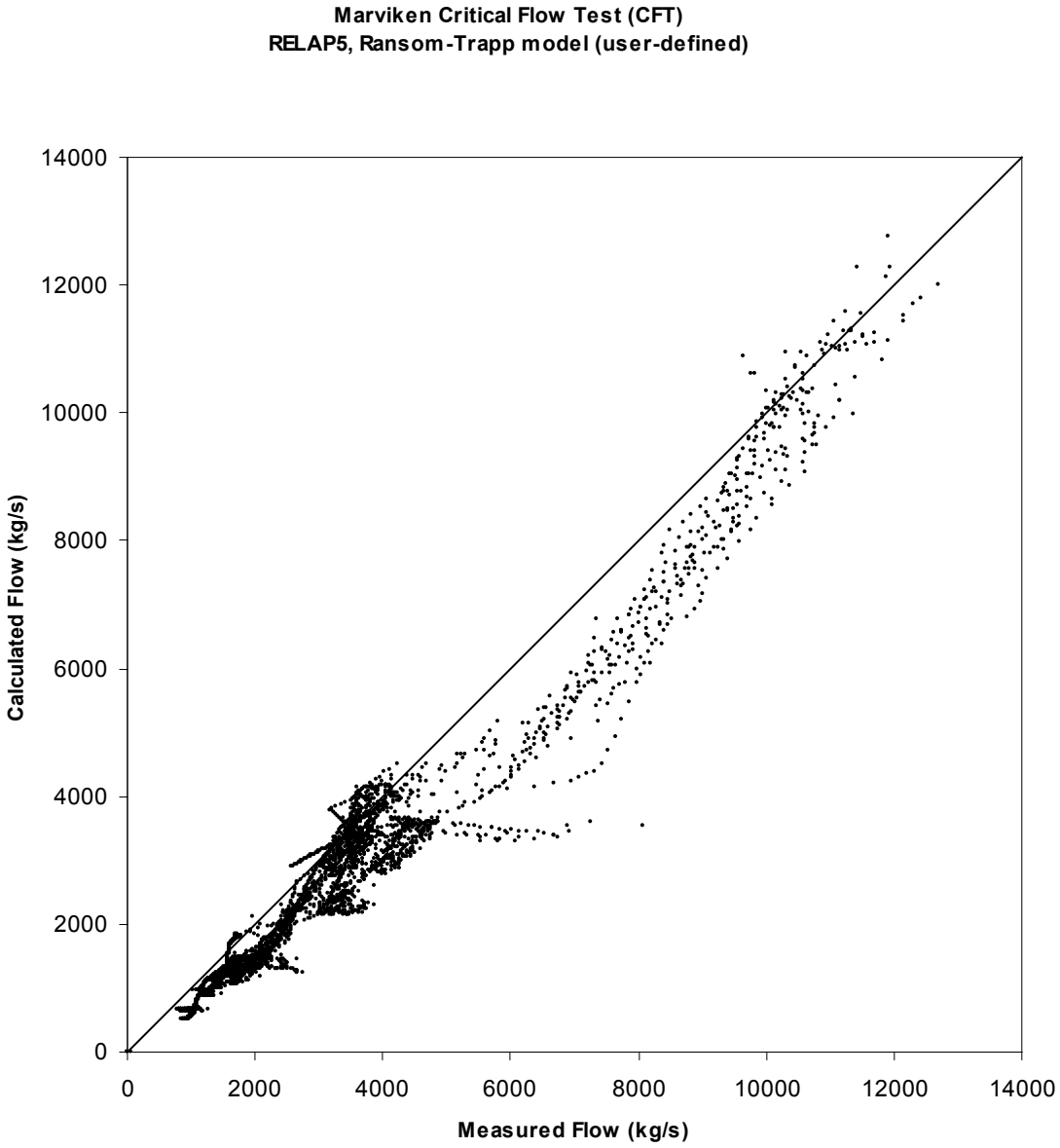

Figure 4.5 Code accuracy, RELAP5 Ransom-Trapp

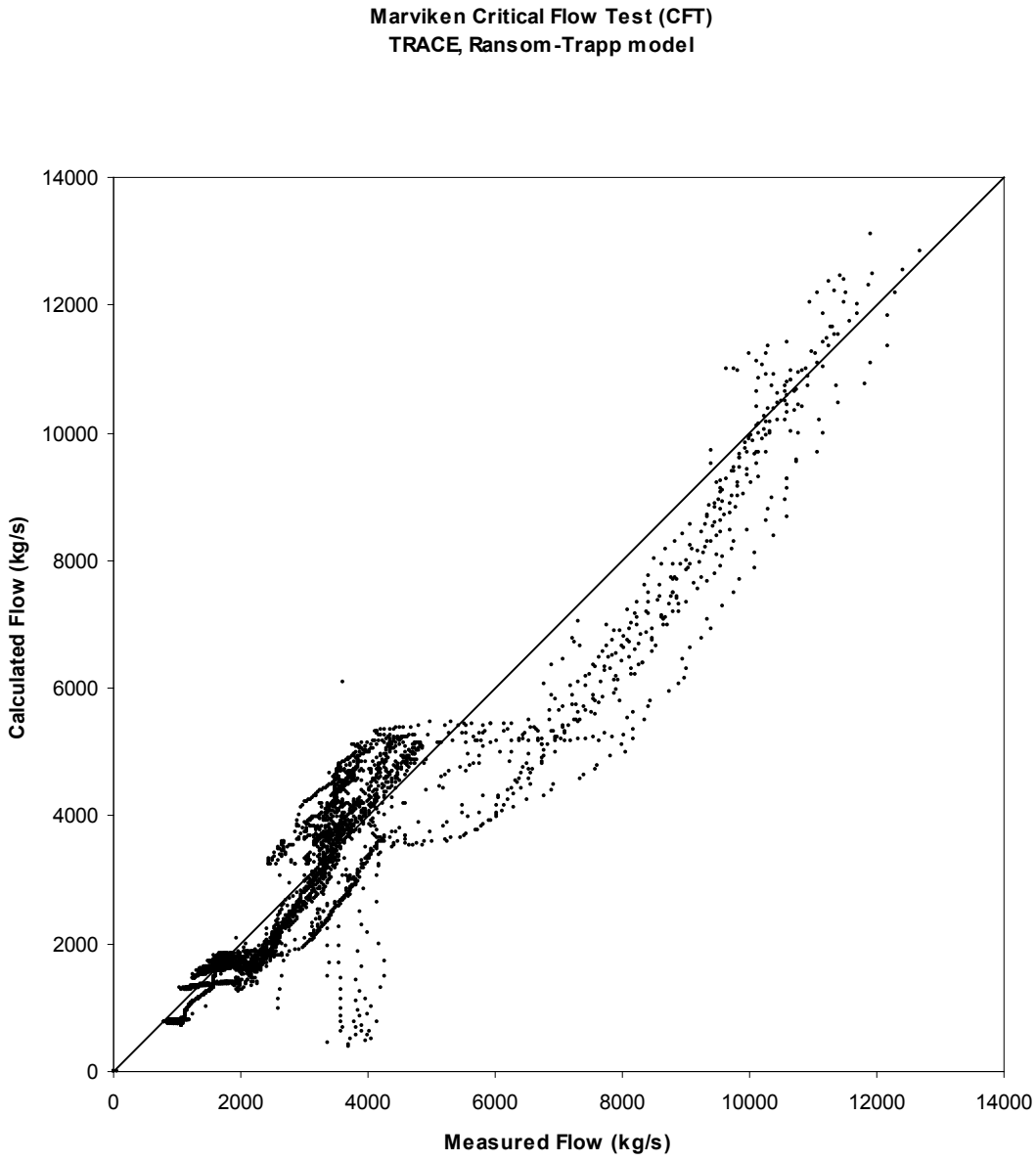

Figure 4.6 Code accuracy, TRACE Ransom-Trapp

4.3.2. Quantitative Code Assessment

The following graphs show relative L1 and L2 norms with respect to Test no and L/D ratio. The special lines indicate the mean value and standard deviation of the computed results for both norms.

Table 5.1 shows values of standard deviation and mean value of two-phase critical models implemented in RELAP5 (R5 H-F and R5 R-T) and TRACE (TR R-T).

Table 4.1 Values of standard deviation and mean value of two-phase critical models implemented in RELAP5 (R5 H-F and R5 R-T) and TRACE (TR R-T)

		R5 H-F	R5 R-T	TR R-T
L1 relative	Standard deviation	0.061	0.068	0.049
	Mean value	0.154	0.183	0.156
L2 relative	Standard deviation	0.082	0.066	0.057
	Mean value	0.190	0.205	0.189

Equations with definitions of L1 and L2 are shown in subsection 3.4.

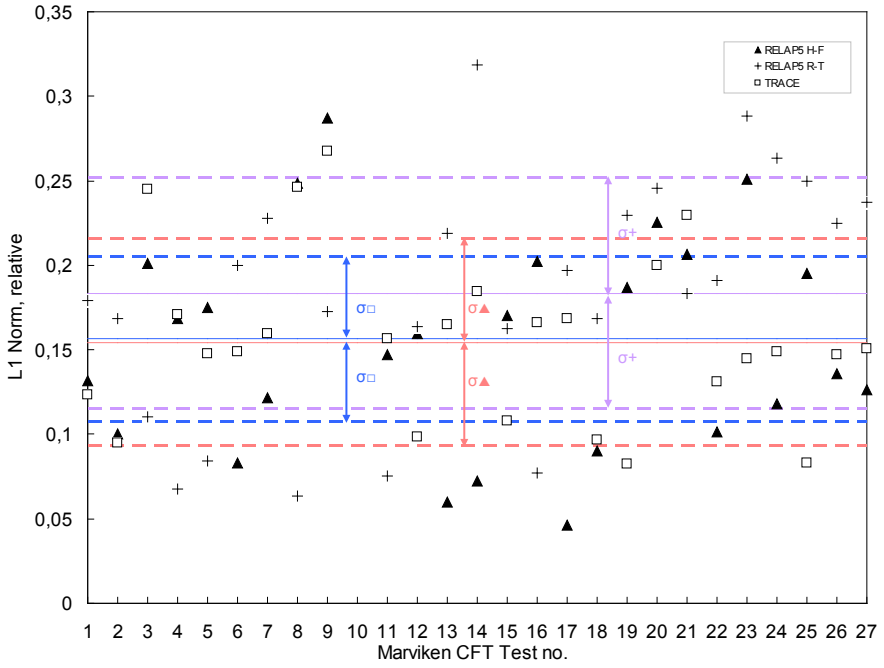

Figure 4.7 Relative L1 norm versus Marviken CFT Test no

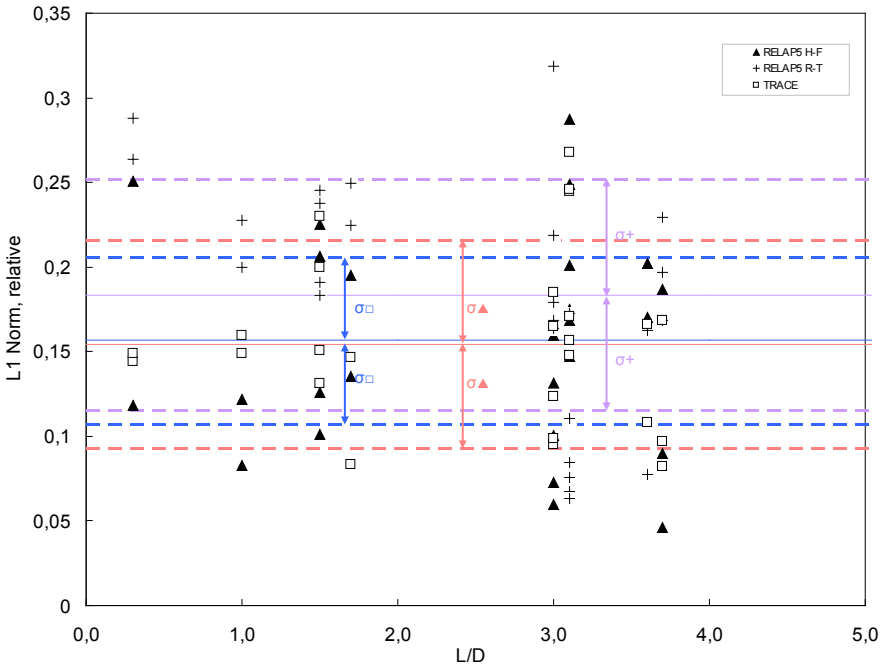

Figure 4.8 Relative L1 norm versus Marviken CFT L/D ratio

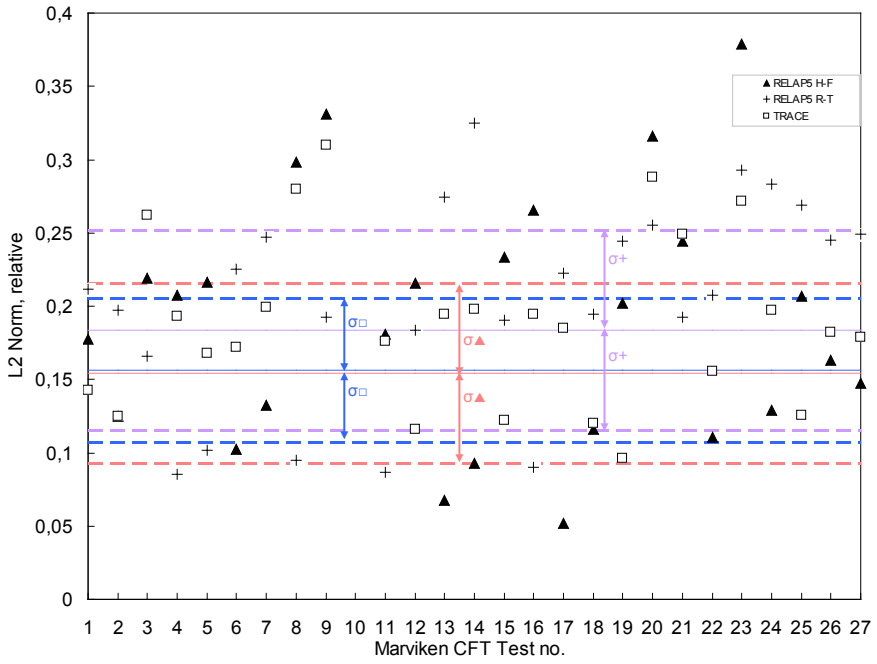

Figure 4.9 Relative L2 norm versus Marviken CFT Test no

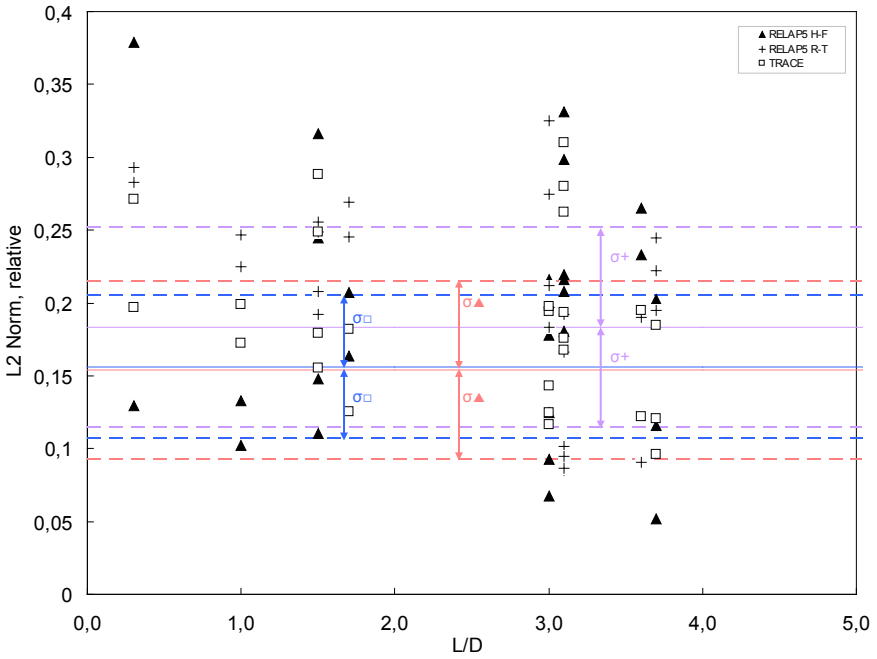

Figure 4.10 Relative L2 norm versus Marviken CFT L/D ratio

The ratio between the number of tests in which Ransom-Trapp gives best results to the number of tests in which the same model gives the worst results is higher for R-T model in TRACE. Table 5.2 provides information about the number of experiments in which certain model gave the best and the worst result.

Table 4.2 Information about the number of experiments in which certain model gave the best and the worst result

	L1 norm			L2 norm		
	R5 H-F	R5 R-T	TR R-T	R5 H-F	R5 R-T	TR R-T
Best	11	7	8	11	9	6
Worst	5	17	4	10	13	3

* Total number of simulations is 26 (Test 10 is missed due to lack of experimental data in [13]).

5. Discussion and Conclusions

The up-to-date thermal-hydraulics models and correlations are of the great importance in computational code environment. Thus, the validation of the systems codes is an important issue. Knowing the behavior of the code under different assumptions and conditions, the more reliable results can be obtained.

The intention of the project was to perform the comprehensive Marviken CFT investigation. This is to build computational models of all tests and conduct a comparison between RELAP5 and TRACE model data and experimental data.

The main conclusions of the study concerns two-phase critical flow models. It was shown that for Marviken CFT experiments RELAP5 Henry-Fauske model gives more accurate results than Ransom-Trapp model.

Additionally, it was found out that Ransom-Trapp implementation in TRACE is better than in RELAP5.

The calculations were performed for a variety of nozzles used in CFT experiment. However, the dependence between length-to-diameter L/D ratio of the nozzle and the calculation's accuracy has not been observed.

6. References

[1] W. Ambrosini, “Critical flow, Flooding and boiling channel instabilities”, Lecture notes on for the course on single and two-phase thermal-hydraulics, University of Pisa, Italy, 2006.

[2] H. Anglart, “Thermo-hydraulics in nuclear energy engineering”, Compendium for students, KTH, Stockholm, 2008.

[3] R.F. Kunz, G.F. Kasmala, J.H. Mahaffy, C.J. Murray, “An Automated Code Assessment Program for Determining System Code Accuracy”, OECD/CSNI Workshop on Advanced Thermal-Hydraulic and Neutronic Codes: Current and Future Applications, Barcelona, Spain, April 10-13, 2000.

[4] F. D’Auria, P. Vigni, “Two-phase critical flow models”, A technical addendum to the CSNI state of the art report on critical flow modeling, Roma, May 1980.

[5] J.A. Trapp, V.H. Ransom, “A chocked-flow calculation criterion for nonhomogeneous, nonequilibrium, two-phase flows”, Idaho National Engineering Laboratory, April 27, 1982.

[6] I. Parzer, “Break model comparison in different RELAP5 versions”, International Conference Nuclear Energy for New Europe 2003, Portoroz, Slovenia, September 8-11, 2003.

[7] RELAP5/MOD3.3 Code Manual, “Volume VII: Summaries and review of independent code assessment reports”, March 2006.

[8] G.A. Mortensen, et al, “RELAP5 status and user problem report”, Fall 2006 CAMP Meeting, Idaho Falls, Idaho, USA, October 2006.

[9] RELAP5/MOD3.3 Code Manual, “Volume II: User’s guide and input requirements”, March 2006.

[10] The Marviken Full Scale Critical Flow Tests report, “Conclusions. MXC-402”, December 1979.

[11] The Marviken Full Scale Critical Flow Tests report, “Summary report. MXC-301”, December 1979.

[12] The Marviken Full Scale Critical Flow Tests report, “Description of the test facility. MXC-101”, December 1979.

[13] CSNI1001 MARVIKEN-CFT. The Nuclear Energy Agency NEA. November 4, 1998.

[14] Marviken CFT data description. The Nuclear Energy Agency NEA.

[15] The Marviken Full Scale Critical Flow Tests report, “Measurement system. MXC-102”, December 1979.

[16] M. Lazor, “Recommended preliminary approach for quantitative code assessment”, Pennsylvania State University, Applied Research Laboratory, December 2004.

[17] R.F. Kunz, G.F. Kasmala, J.H. Mahaffy, “Automated Code Assessment Program: Technique selection and mathematical prescription”, Pennsylvania State University, Applied Research Laboratory, April 1998.

[18] Ö. Rosdahl, D. Caraher, “Assessment of RELAP/MOD2 against Critical Flow Data from Marviken Tests JIT 11 and CFT 21”, NUREG/IA-0007, US Nuclear Regulatory Commission, September, 1986.

[19] A. Ylönen, “Large break blowdown test facility study”, Master thesis, Lappeenranta University of Technology, Lappeenranta, Finland, March 3, 2008.

[20] TRACE v5.0 User’s Manual, 2008-10-07.

[21] TRAC-PF1/MOD2 Volume I. Theory manual, 1993-07-21.

7. Appendix A: Summary of the Initial and Final Conditions

1	Test No.	1	2	3	4	5
2	Data of test performance	1978 01-19	1978 02-02	1978 02-24	1978 03-09	1978 03-21
3	Steam dome pressure ~ MPa	4.94	4.98	5.02	4.94	4.06
4	Saturation temperature ~°C	263	264	264	264	251
5	Degree of nominal subcooling in the lower vessel (relative to steam dome saturation temperature)~°C	17-23	38	15-22	37	33
6	Min. fluid temperature in the vessel ~°C	238	226	243	224	218
7	Initial temperature at nozzle inlet ~°C	226	213	223	201	205
8	Mass of water and steam ~°C (incl the water in the discharge pipe)	287	284	274	286	286
9	Mass of steam ~ Mg	1.7	2.0	2.2	1.9	1.6
10	Mass of saturated water ~ Mg	114	104	100.5	109	110
11	Initial level in the vessel ~ m	17.84	17.41	17.06	17.59	17.44
12	Final level in the vessel ~ m	3.58	3.35	2.8	<0.74	<1.1
13	Nominal elevation of transition zone* = m ± 0.5	9-11	8-11	7-9.5	8-10.5	8-10.5
14	Test period** ~ s	108	93	42	49	52
1	Test No	6	7	8	9	10
2	Data of test performance	1978 04-13	1978 04-27	1978 05-18	1978 06-01	1978 06-20
3	Steam dome pressure ~ MPa	4.95	5.01	4.95	5.02	4.97
4	Saturation temperature ~°C	263	264	263	264	163.5
5	Degree of nominal subcooling in the lower vessel (relative to steam dome saturation temperature)~°C	31	18	35	2	3
6	Min. fluid temperature in the vessel ~°C	231	246	225	262	260
7	Initial temperature at nozzle inlet ~°C	219	229	200	243	242
8	Mass of water and steam ~°C (incl the water in the discharge pipe)	289	286	285	286	279
9	Mass of steam ~ Mg	1.7	1.7	1.9	1.6	1.8
10	Mass of saturated water ~ Mg	113	125	108	256	208
11	Initial level in the vessel ~ m	17.81	17.86	17.51	18.15	17.66

12	Final level in the vessel ~ m	3.39	4.36	<0.74	<0.74	<0.74
13	Nominal elevation of transition zone* = m ± 0.5	7.5-10.5	8-9.5	8-10	III	III
14	Test period** ~ s	87	87	49	66	64
1	Test No	11	12	13	14	15
2	Data of test performance	1978 08-17	1978 08-29	1978 09-12	1978 09-21	1978 11-01
3	Steam dome pressure ~ MPa	4.97	5.00	5.09	4.97	5.04
4	Saturation temperature ~°C	264	264	265	264	264
5	Degree of nominal subcooling in the lower vessel (relative to steam dome saturation temperature)~°C	35	33	31	3	31
6	Min. fluid temperature in the vessel ~°C	228	231	232	260	233
7	Initial temperature at nozzle inlet ~°C	202	215	170	170	177
8	Mass of water and steam ~°C (incl the water in the discharge pipe)	287	285	282	286	327
9	Mass of steam ~ Mg	1.8	1.9	1.9	1.6	0.6
10	Mass of saturated water ~ Mg	110	108	132	167	73.1
11	Initial level in the vessel ~ m	17.63	17.52	17.52	18.10	19.93
12	Final level in the vessel ~ m	<0.74	<0.74	5.33	8.70	<0.74
13	Nominal elevation of transition zone* = m ± 0.5	7.5-10	7.5-10.5	7-10	III	12.5-14
14	Test period** ~ s	48	126	148	146	55
1	Test No	16	17	18	19	20
2	Data of test performance	1978 11-16	1978 11-30	1978 12-12	1979 01-09	1979 01-25
3	Steam dome pressure ~ MPa	5.00	4.94	5.02	5.06	4.99
4	Saturation temperature ~°C	264	263	264	265	264
5	Degree of nominal subcooling in the lower vessel (relative to steam dome saturation temperature)~°C	33	31	32	4	7
6	Min. fluid temperature in the vessel ~°C	231	232	232	261	257
7	Initial temperature at nozzle inlet ~°C	180	174	174	167	187
8	Mass of water and steam ~°C (incl the water in the discharge pipe)	286	329	281	267	262
9	Mass of steam ~ Mg	1.9	0.7	2.0	2.23	2.40
10	Mass of saturated water ~ Mg	102	38.8	97.3	262.6	257.3
11	Initial level in the vessel ~ m	17.60	19.85	17.30	16.99	16.65

12	Final level in the vessel ~ m	<0.74	6.2	3.8	6.5	<0.74
13	Nominal elevation of transition zone* = m ± 0.5	7.5-11.5	15.5-16.5	8-11	III	III
14	Test period** ~ s	49	90	87	87	58
1	Test No	21	22	23	24	25
2	Data of test performance	1979 02-08	1979 02-27	1979 03-13	1979 03-29	1979 04-19
3	Steam dome pressure ~ MPa	4.94	4.93	4.96	4.96	4.92
4	Saturation temperature ~°C	263	263	263	263	263
5	Degree of nominal subcooling in the lower vessel (relative to steam dome saturation temperature)~°C	33	52	3	33	6
6	Min. fluid temperature in the vessel ~°C	230	211	260	230	257
7	Initial temperature at nozzle inlet ~°C	184	168	19	27	189
8	Mass of water and steam ~°C (incl the water in the discharge pipe)	330	334	314	330	313
9	Mass of steam ~ Mg	0.60	0.75	0.65	0.63	0.70
10	Mass of saturated water ~ Mg	48.9	35.7	310.7	39.4	309.8
11	Initial level in the vessel ~ m	19.95	19.64	19.85	19.88	19.73
12	Final level in the vessel ~ m	<0.74	<0.74	<0.74	<0.74	<0.74
13	Nominal elevation of transition zone* = m ± 0.5	15.5-17	15.5-17	III	15.5-17	III
14	Test period** ~ s	60	48	69	54	88
1	Test No	26	27			
2	Data of test performance	1979 05-03	1979 05-22			
3	Steam dome pressure ~ MPa	4.91	4.91			
4	Saturation temperature ~°C	263	263			
5	Degree of nominal subcooling in the lower vessel (relative to steam dome saturation temperature)~°C	34	33			
6	Min. fluid temperature in the vessel ~°C	229	230			
7	Initial temperature at nozzle inlet ~°C	135	167			
8	Mass of water and steam ~°C (incl the water in the discharge pipe)	320	329			
9	Mass of steam ~ Mg	0.92	0.66			
10	Mass of saturated water ~ Mg	38.8	46.9			
11	Initial level in the vessel ~ m	19.31	19.82			

12	Final level in the vessel ~ m	<0.74	<0.74
13	Nominal elevation of transition zone* = m ± 0.5	15.5-17	15.5-17
14	Test period** ~ s	147	59

* III indicates that little or no transition zone was present; ** Test period is the time from test initiation to when steam enters the discharge pipe (or the ball valve begins to close).

8. Appendix B: Data Channel Outputs Used in the Computational Model

Data channel	Type	Elevation level, m
001M101	Pressure	23.13
001M104	Pressure	0.53
001M401	Temperature	20.54
001M501	Temperature	19.56
001M502	Temperature	18.59
001M503	Temperature	17.64
001M504	Temperature	16.67
001M505	Temperature	15.69
001M506	Temperature	14.71
001M507	Temperature	13.75
001M508	Temperature	12.78
001M509	Temperature	11.81
001M510	Temperature	10.84
001M511	Temperature	9.86
001M512	Temperature	8.88
001M514	Temperature	6.94
001M515	Temperature	5.97
001M516	Temperature	5.00
001M517	Temperature	4.03
001M419	Temperature	3.94
001M518	Temperature	3.040

001M519	Temperature	2.08
001M520	Temperature	1.11
001M402	Temperature	0.74
002M107	Pressure	-0.630
003M108	Pressure	-2.730
004M109	Pressure	-4.868
002M403	Temperature	-0.630
003M404	Temperature	-2.730
004M405	Temperature	-4.868
004M532	Temperature	-5.543

9. Appendix C: Flow Rate Comparisons

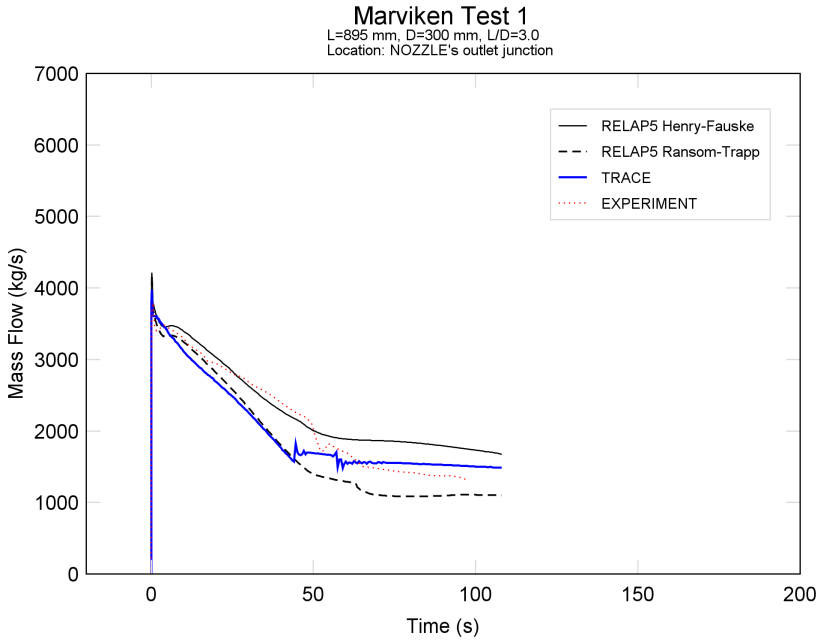

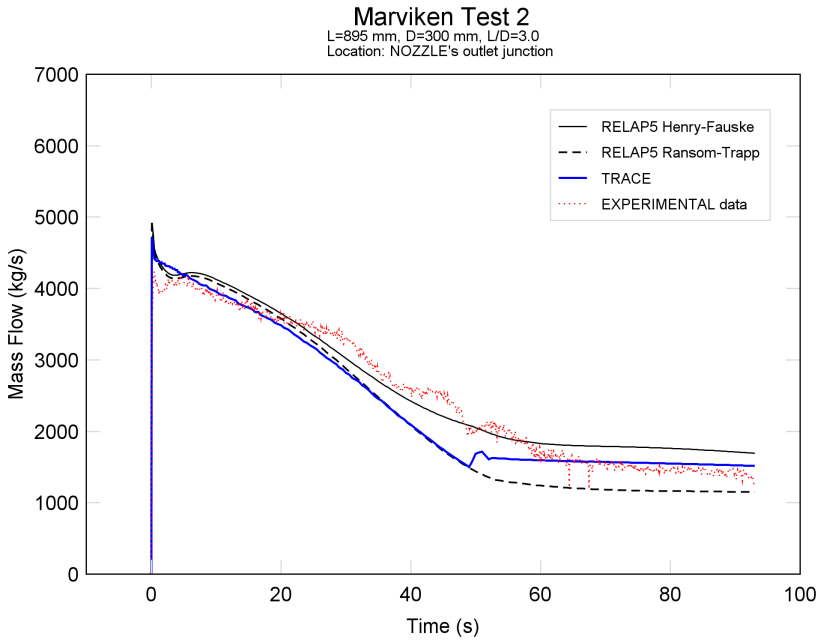

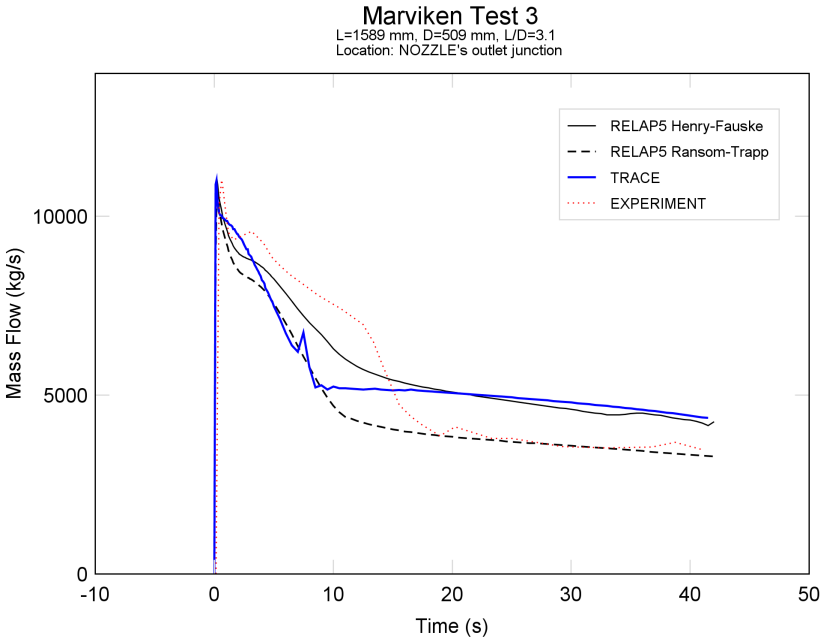
Marviken Test 3
L=1589 mm, D=509 mm, L/D=3.1
Location: NOZZLE's outlet junction
RELAP5 Henry-Fauske
RELAP5 Ransom-Trapp
TRACE
EXPERIMENT
Mass Flow (kg/s)
Time (s)
0
5000
10000
-10
0
10
20
30
40
50

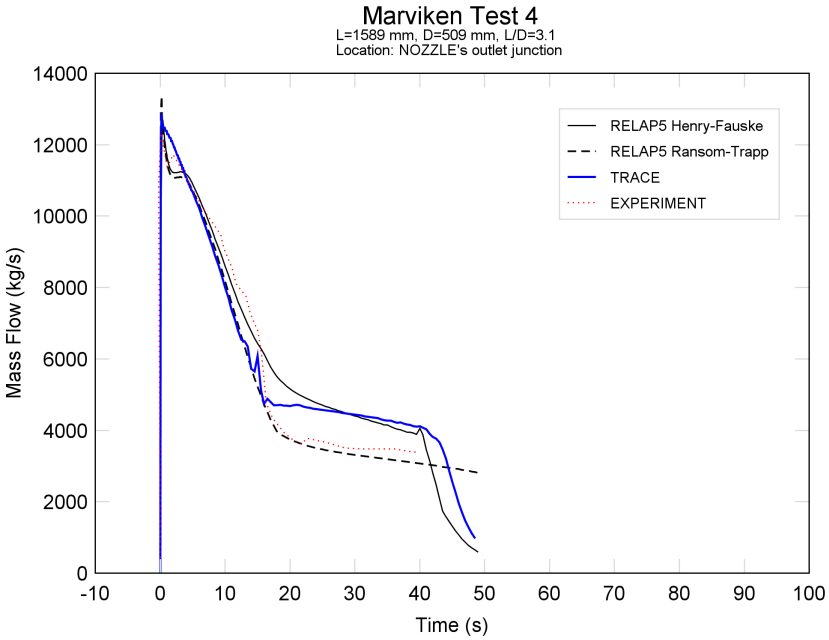
Marviken Test 4
L=1589 mm, D=509 mm, L/D=3.1
Location: NOZZLE's outlet junction
RELAP5 Henry-Fauske
RELAP5 Ransom-Trapp
TRACE
EXPERIMENT
Mass Flow (kg/s)
Time (s)
0
2000
4000
6000
8000
10000
12000
14000
-10
0
10
20
30
40
50
60
70
80
90
100

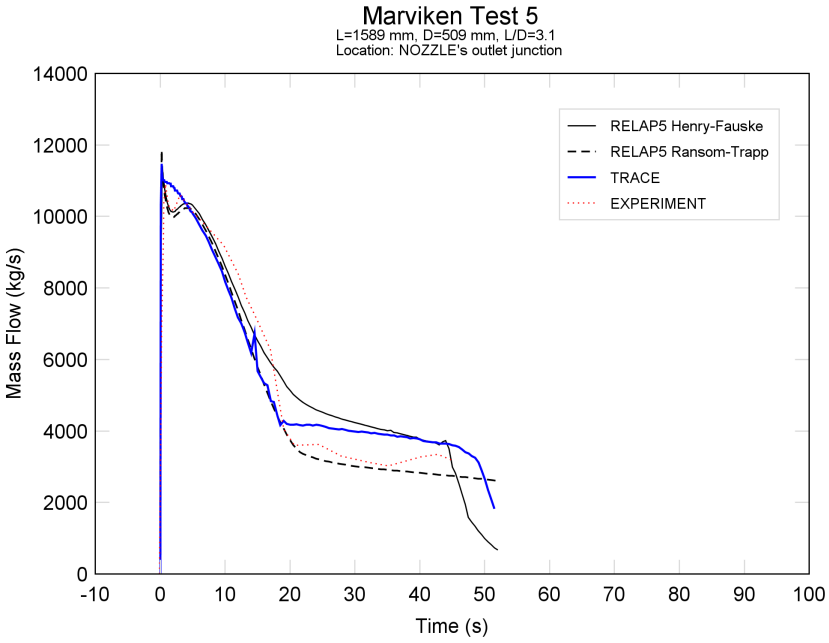
Marviken Test 5
L=1589 mm, D=509 mm, L/D=3.1
Location: NOZZLE's outlet junction
Mass Flow (kg/s)
Time (s)
RELAP5 Henry-Fauske
RELAP5 Ransom-Trapp
TRACE
EXPERIMENT

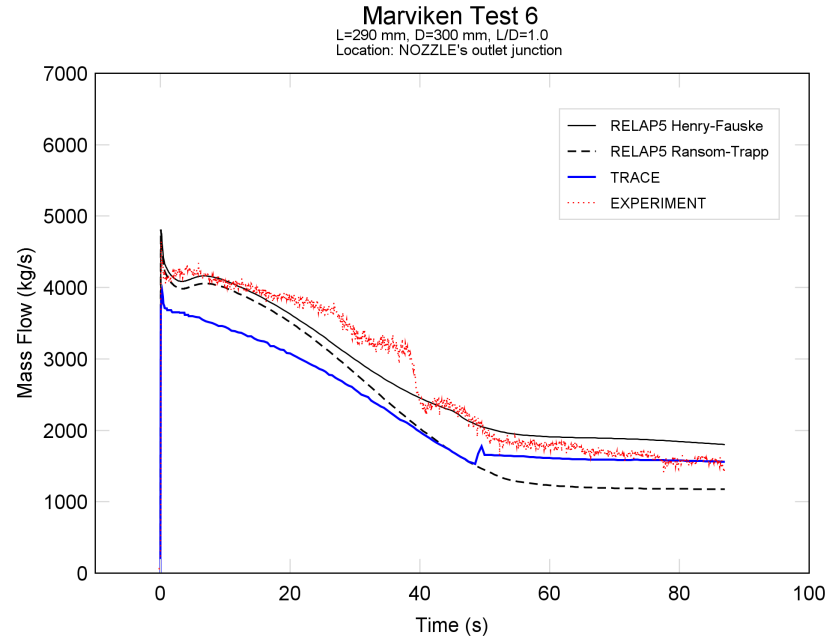
Marviken Test 6
L=290 mm, D=300 mm, L/D=1.0
Location: NOZZLE's outlet junction
Mass Flow (kg/s)
Time (s)
RELAP5 Henry-Fauske
RELAP5 Ransom-Trapp
TRACE
EXPERIMENT

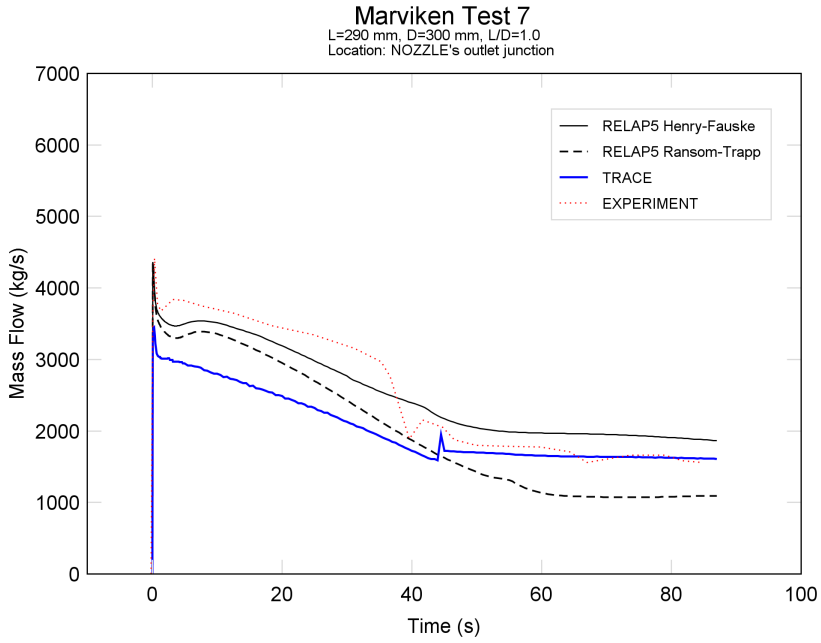
Marviken Test 7
L=290 mm, D=300 mm, L/D=1.0
Location: NOZZLE's outlet junction
RELAP5 Henry-Fauske
RELAP5 Ransom-Trapp
TRACE
EXPERIMENT
Mass Flow (kg/s)
Time (s)
0
1000
2000
3000
4000
5000
6000
7000
0
20
40
60
80
100

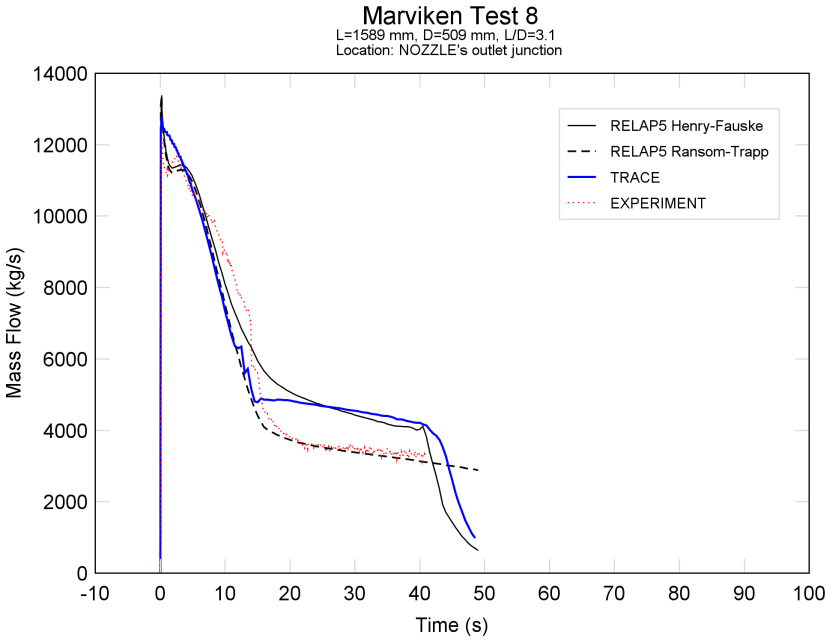
Marviken Test 8
L=1589 mm, D=509 mm, L/D=3.1
Location: NOZZLE's outlet junction
RELAP5 Henry-Fauske
RELAP5 Ransom-Trapp
TRACE
EXPERIMENT
Mass Flow (kg/s)
Time (s)
0
2000
4000
6000
8000
10000
12000
14000
-10
0
10
20
30
40
50
60
70
80
90
100

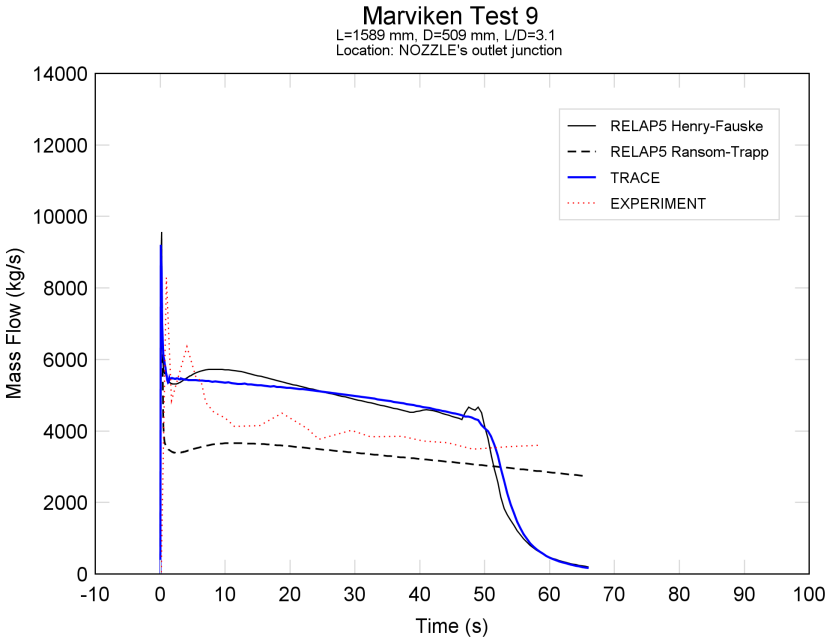
Marviken Test 9
L=1589 mm, D=509 mm, L/D=3.1
Location: NOZZLE's outlet junction
Mass Flow (kg/s)
Time (s)
RELAP5 Henry-Fauske
RELAP5 Ransom-Trapp
TRACE
EXPERIMENT
14000
12000
10000
8000
6000
4000
2000
0
-10
0
10
20
30
40
50
60
70
80
90
100

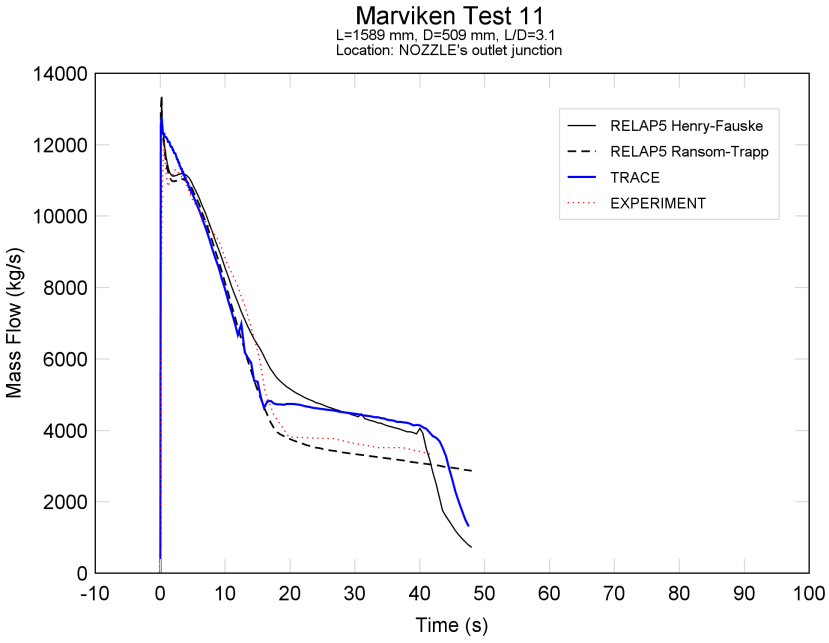
Marviken Test 11
L=1589 mm, D=509 mm, L/D=3.1
Location: NOZZLE's outlet junction
Mass Flow (kg/s)
Time (s)
RELAP5 Henry-Fauske
RELAP5 Ransom-Trapp
TRACE
EXPERIMENT
14000
12000
10000
8000
6000
4000
2000
0
-10
0
10
20
30
40
50
60
70
80
90
100

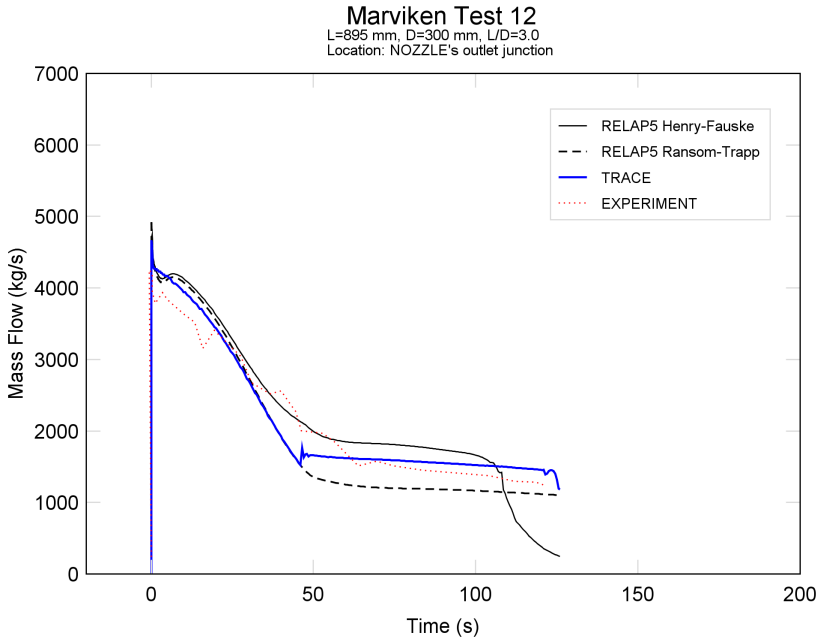
Marviken Test 12
L=895 mm, D=300 mm, L/D=3.0
Location: NOZZLE's outlet junction
RELAP5 Henry-Fauske
RELAP5 Ransom-Trapp
TRACE
EXPERIMENT
Mass Flow (kg/s)
Time (s)
0
1000
2000
3000
4000
5000
6000
7000
0
50
100
150
200

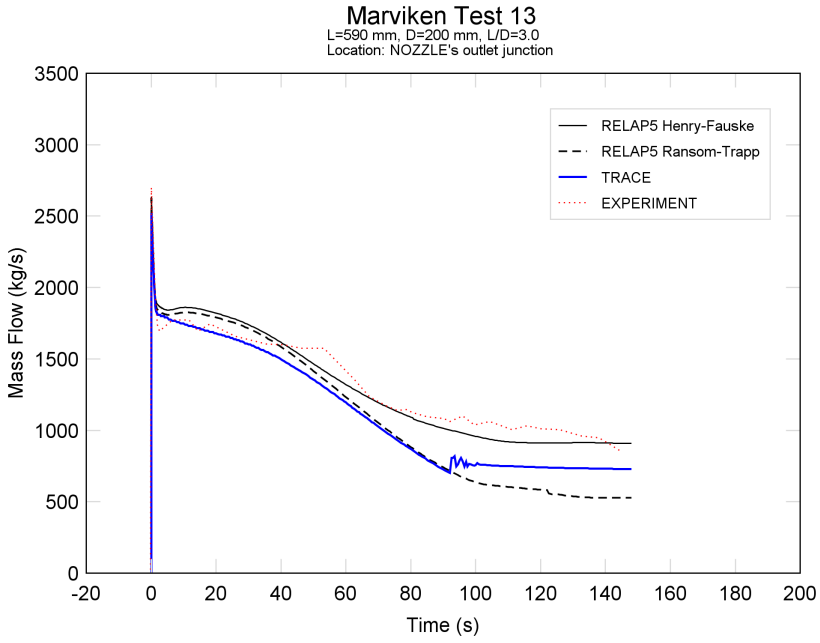
Marviken Test 13
L=590 mm, D=200 mm, L/D=3.0
Location: NOZZLE's outlet junction
RELAP5 Henry-Fauske
RELAP5 Ransom-Trapp
TRACE
EXPERIMENT
Mass Flow (kg/s)
Time (s)
0
500
1000
1500
2000
2500
3000
3500
-20
0
20
40
60
80
100
120
140
160
180
200

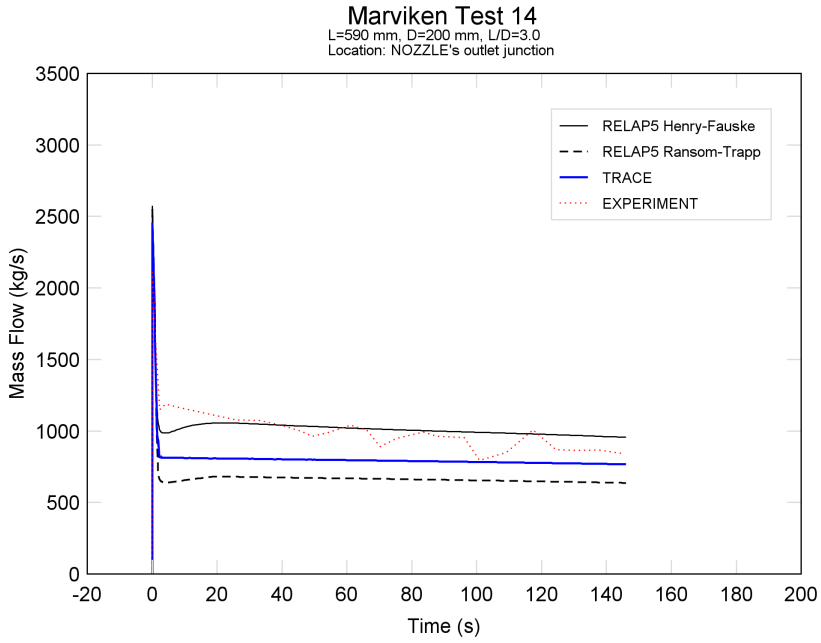
Marviken Test 14
L=590 mm, D=200 mm, L/D=3.0
Location: NOZZLE's outlet junction
Mass Flow (kg/s)
Time (s)
RELAP5 Henry-Fauske
RELAP5 Ransom-Trapp
TRACE
EXPERIMENT
3500
3000
2500
2000
1500
1000
500
0
-20
0
20
40
60
80
100
120
140
160
180
200

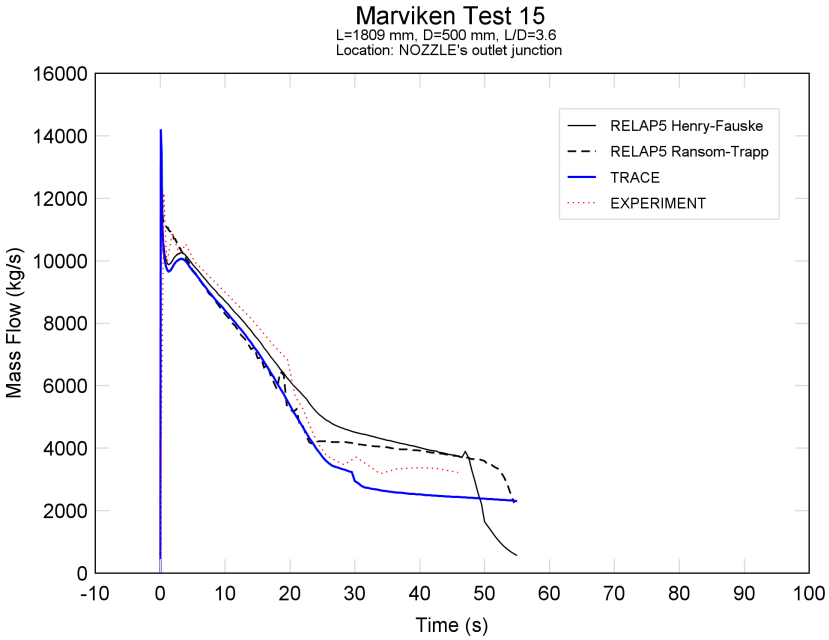
Marviken Test 15
L=1809 mm, D=500 mm, L/D=3.6
Location: NOZZLE's outlet junction
Mass Flow (kg/s)
Time (s)
RELAP5 Henry-Fauske
RELAP5 Ransom-Trapp
TRACE
EXPERIMENT
16000
14000
12000
10000
8000
6000
4000
2000
0
-10
0
10
20
30
40
50
60
70
80
90
100

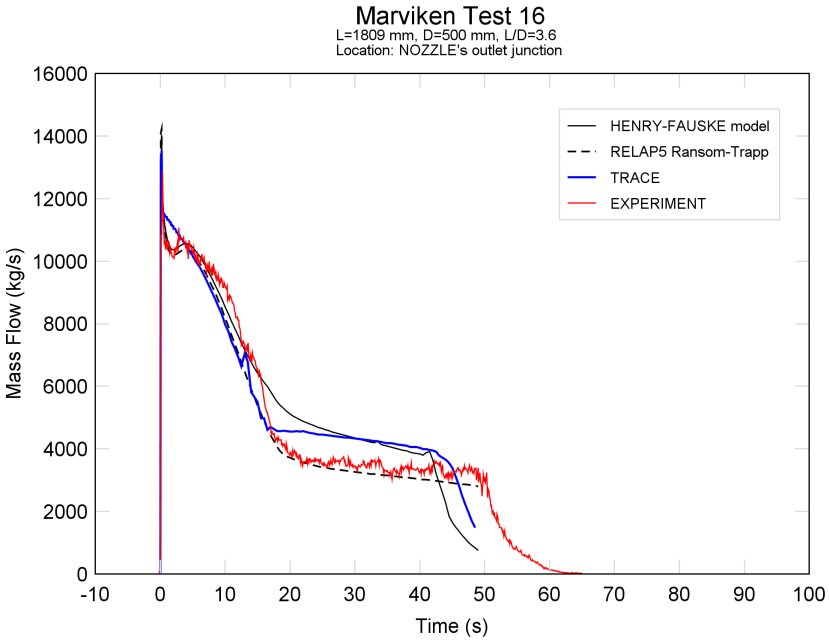
Marviken Test 16
L=1809 mm, D=500 mm, L/D=3.6
Location: NOZZLE's outlet junction
HENRY-FAUSKE model
RELAP5 Ransom-Trapp
TRACE
EXPERIMENT
Mass Flow (kg/s)
Time (s)
16000
14000
12000
10000
8000
6000
4000
2000
0
-10
0
10
20
30
40
50
60
70
80
90
100

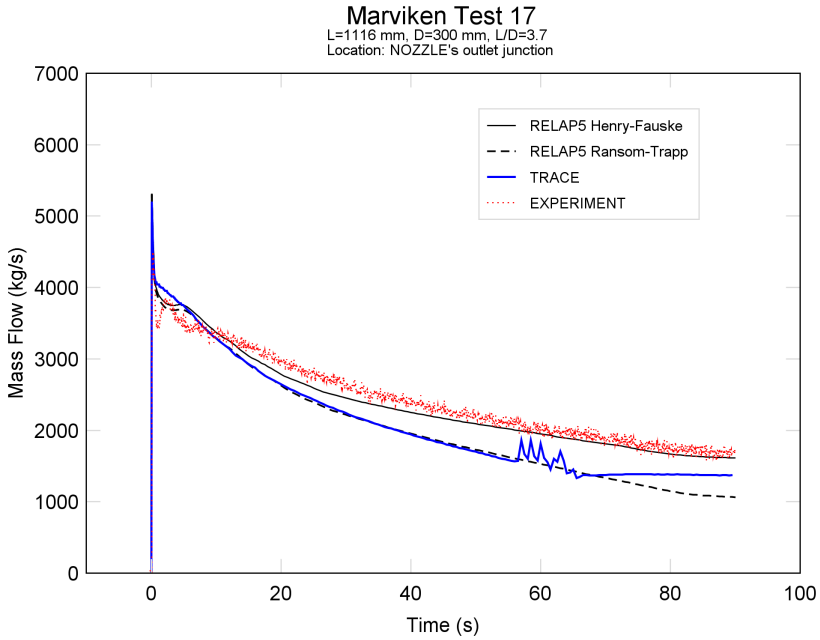
Marviken Test 17
L=1116 mm, D=300 mm, L/D=3.7
Location: NOZZLE's outlet junction
RELAP5 Henry-Fauske
RELAP5 Ransom-Trapp
TRACE
EXPERIMENT
Mass Flow (kg/s)
Time (s)
7000
6000
5000
4000
3000
2000
1000
0
0
20
40
60
80
100

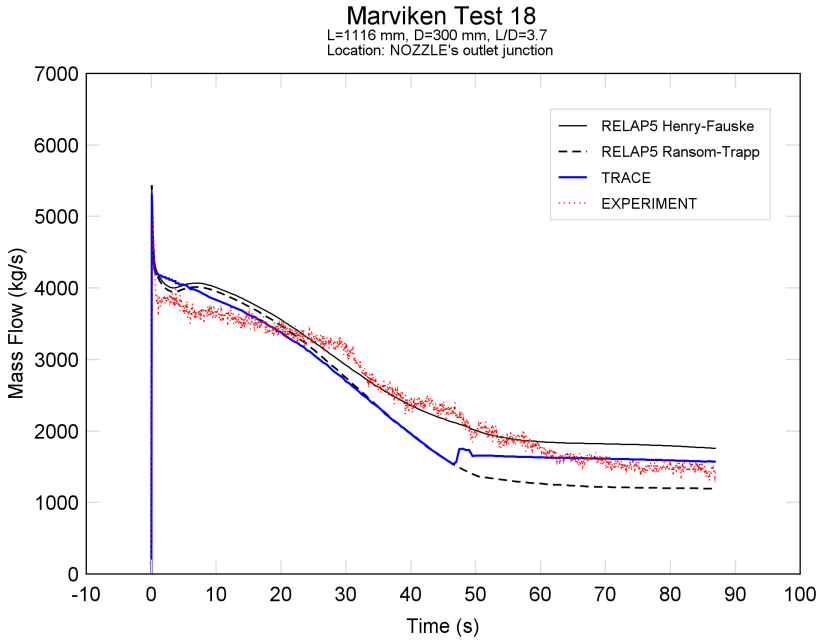
Marviken Test 18
L=1116 mm, D=300 mm, L/D=3.7
Location: NOZZLE's outlet junction
RELAP5 Henry-Fauske
RELAP5 Ransom-Trapp
TRACE
EXPERIMENT
Mass Flow (kg/s)
Time (s)
7000
6000
5000
4000
3000
2000
1000
0
-10
0
10
20
30
40
50
60
70
80
90
100

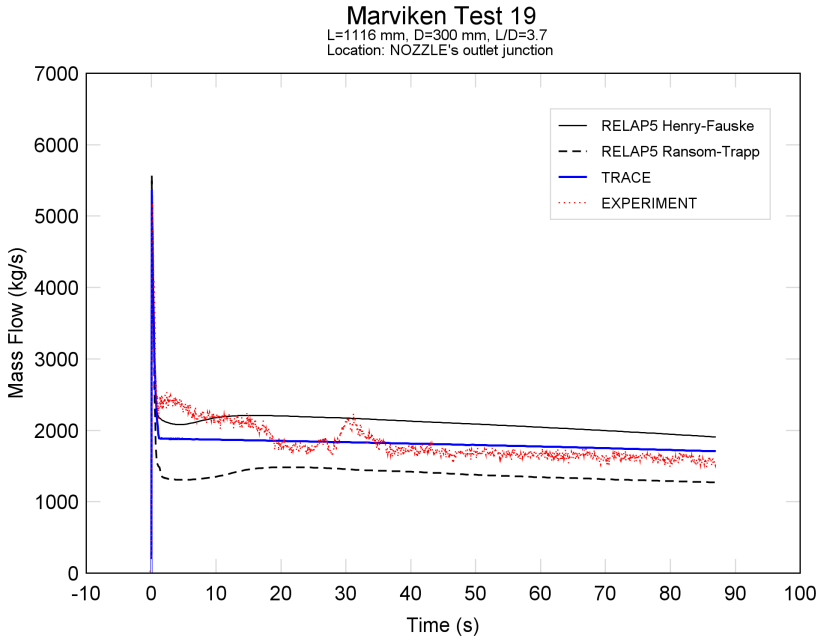
Marviken Test 19
L=1116 mm, D=300 mm, L/D=3.7
Location: NOZZLE's outlet junction
RELAP5 Henry-Fauske
RELAP5 Ransom-Trapp
TRACE
EXPERIMENT
Mass Flow (kg/s)
Time (s)
7000
6000
5000
4000
3000
2000
1000
0
-10
0
10
20
30
40
50
60
70
80
90
100

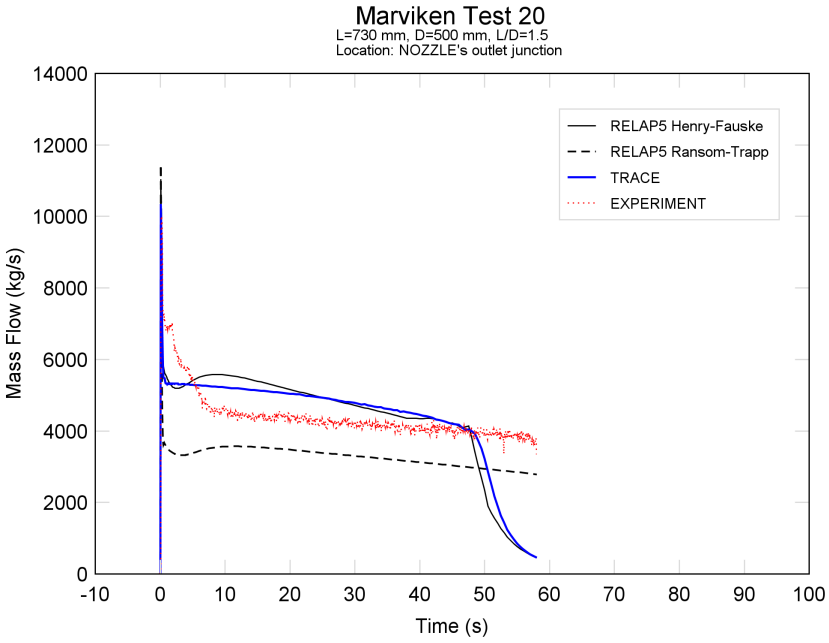
Marviken Test 20
L=730 mm, D=500 mm, L/D=1.5
Location: NOZZLE's outlet junction
Mass Flow (kg/s)
Time (s)
RELAP5 Henry-Fauske
RELAP5 Ransom-Trapp
TRACE
EXPERIMENT
14000
12000
10000
8000
6000
4000
2000
0
-10
0
10
20
30
40
50
60
70
80
90
100

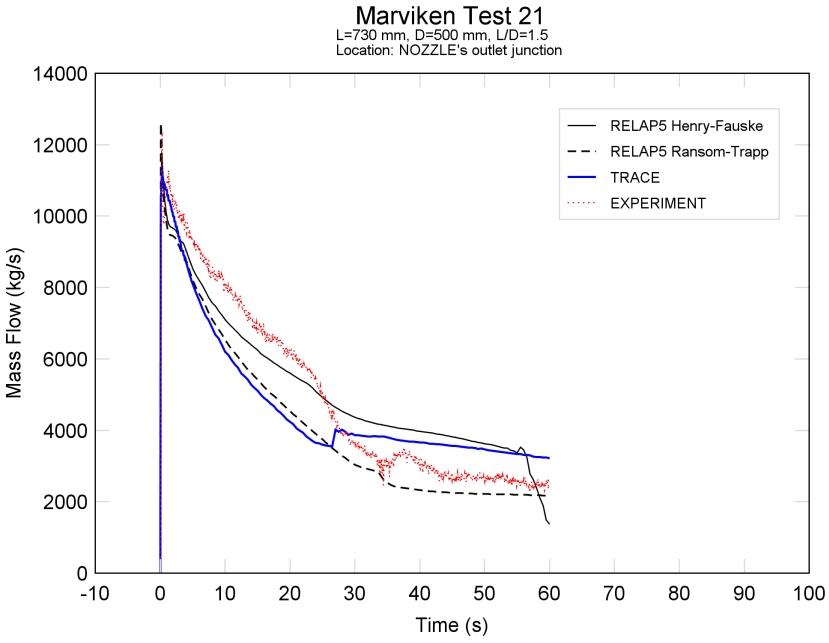
Marviken Test 21
L=730 mm, D=500 mm, L/D=1.5
Location: NOZZLE's outlet junction
Mass Flow (kg/s)
Time (s)
RELAP5 Henry-Fauske
RELAP5 Ransom-Trapp
TRACE
EXPERIMENT
14000
12000
10000
8000
6000
4000
2000
0
-10
0
10
20
30
40
50
60
70
80
90
100

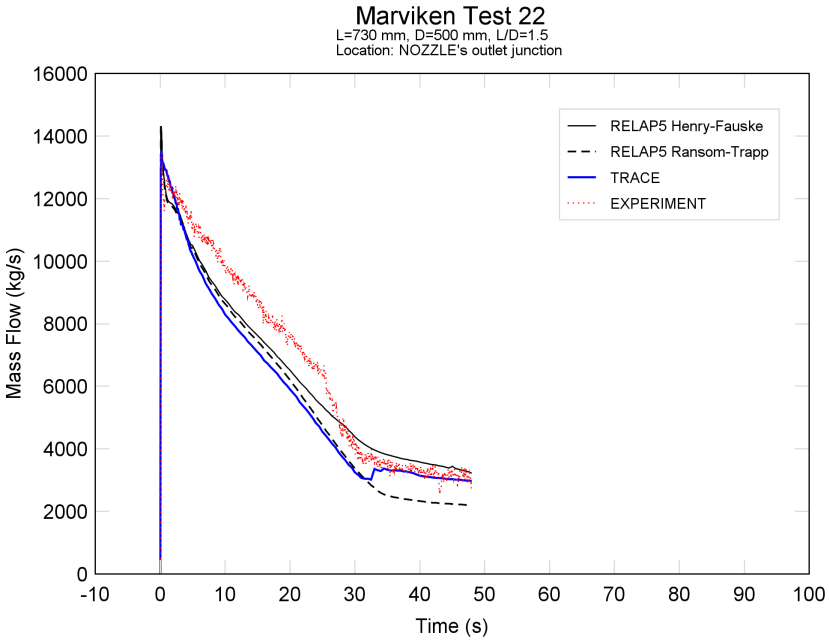
Marviken Test 22
L=730 mm, D=500 mm, L/D=1.5
Location: NOZZLE's outlet junction
RELAP5 Henry-Fauske
RELAP5 Ransom-Trapp
TRACE
EXPERIMENT
Mass Flow (kg/s)
Time (s)
16000
14000
12000
10000
8000
6000
4000
2000
0
-10
0
10
20
30
40
50
60
70
80
90
100

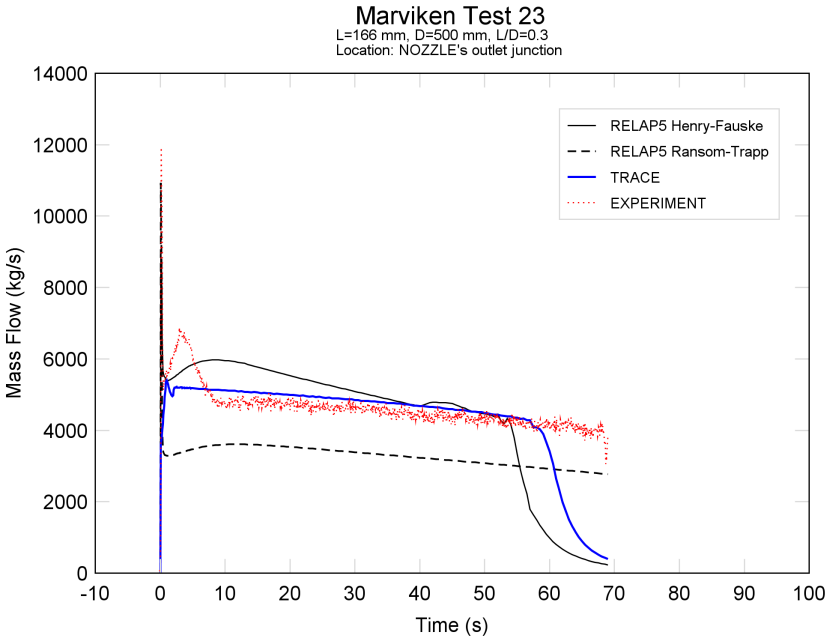
Marviken Test 23
L=166 mm, D=500 mm, L/D=0.3
Location: NOZZLE's outlet junction
RELAP5 Henry-Fauske
RELAP5 Ransom-Trapp
TRACE
EXPERIMENT
Mass Flow (kg/s)
Time (s)
14000
12000
10000
8000
6000
4000
2000
0
-10
0
10
20
30
40
50
60
70
80
90
100

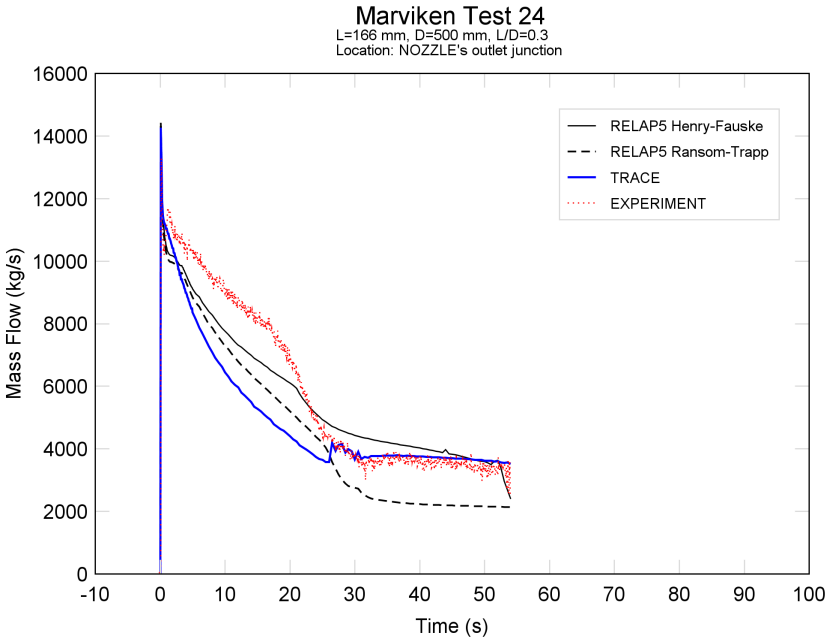
Marviken Test 24
L=166 mm, D=500 mm, L/D=0.3
Location: NOZZLE's outlet junction
Mass Flow (kg/s)
Time (s)
RELAP5 Henry-Fauske
RELAP5 Ransom-Trapp
TRACE
EXPERIMENT

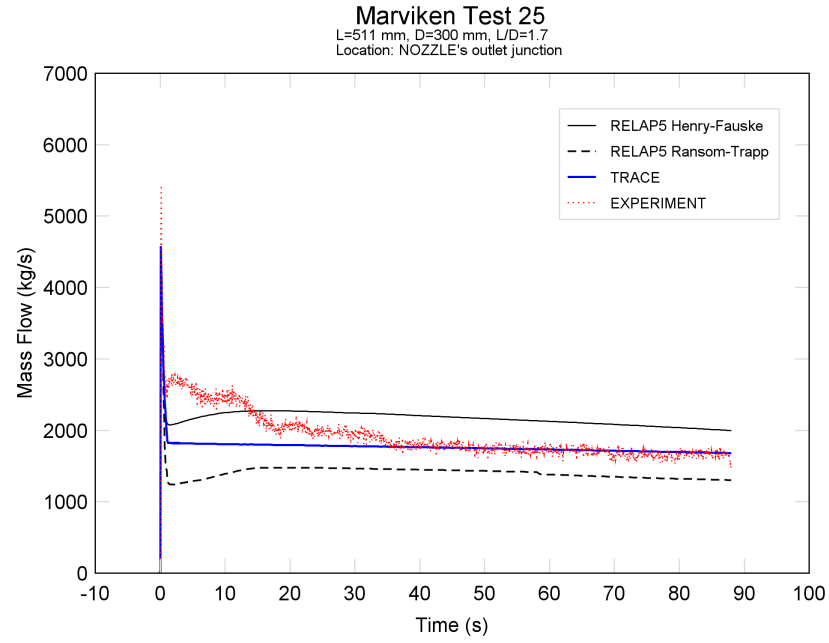
Marviken Test 25
L=511 mm, D=300 mm, L/D=1.7
Location: NOZZLE's outlet junction
Mass Flow (kg/s)
Time (s)
RELAP5 Henry-Fauske
RELAP5 Ransom-Trapp
TRACE
EXPERIMENT

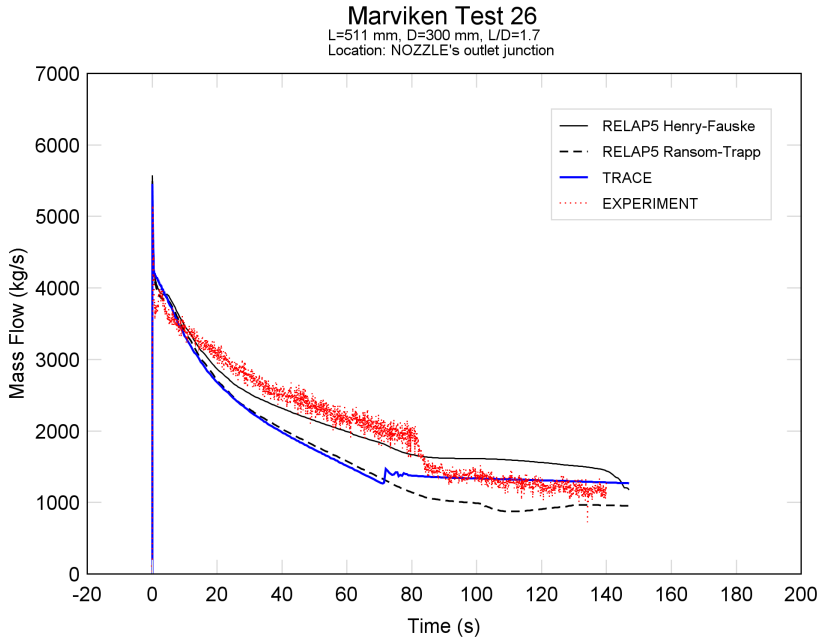
Marviken Test 26
L=511 mm, D=300 mm, L/D=1.7
Location: NOZZLE's outlet junction
RELAP5 Henry-Fauske
RELAP5 Ransom-Trapp
TRACE
EXPERIMENT
Mass Flow (kg/s)
Time (s)
7000
6000
5000
4000
3000
2000
1000
0
-20
0
20
40
60
80
100
120
140
160
180
200

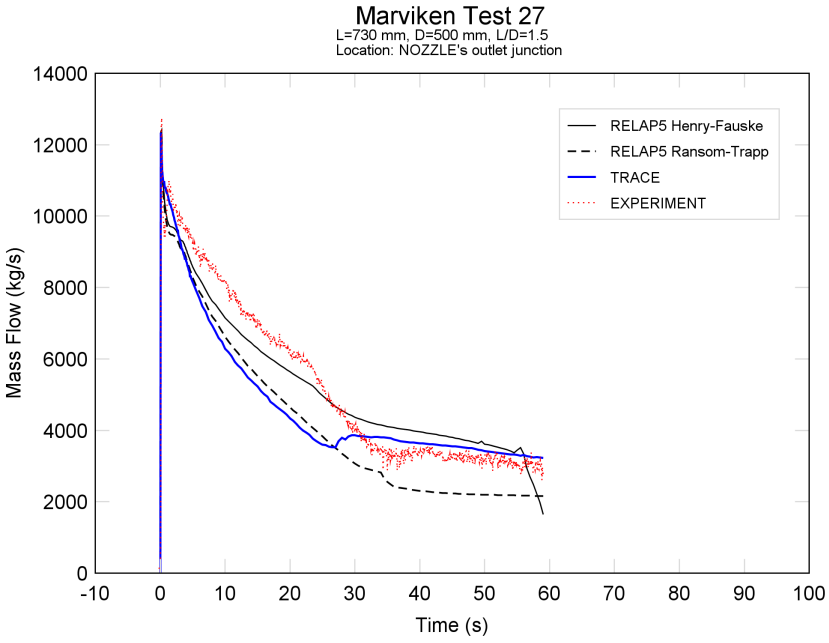
Marviken Test 27
L=730 mm, D=500 mm, L/D=1.5
Location: NOZZLE's outlet junction
RELAP5 Henry-Fauske
RELAP5 Ransom-Trapp
TRACE
EXPERIMENT
Mass Flow (kg/s)
Time (s)
14000
12000
10000
8000
6000
4000
2000
0
-10
0
10
20
30
40
50
60
70
80
90
100

NRC FORM 335
(9-2004)
NRCMD 3.7

U.S. NUCLEAR REGULATORY COMMISSION

BIBLIOGRAPHIC DATA SHEET

(See instructions on the reverse)

1. REPORT NUMBER
(Assigned by NRC, Add Vol., Supp., Rev., and Addendum Numbers, if any.)
NUREG/IA-0401

2. TITLE AND SUBTITLE
Assessment of Two-Phase Critical Flow Models Performance in RELAP5 and TRACE against Marviken Critical Flow Tests

3. DATE REPORT PUBLISHED
MONTH: February
YEAR: 2012

4. FIN OR GRANT NUMBER

5. AUTHOR(S)
Lukasz Sokolowski, Tomasz Kozlowski

6. TYPE OF REPORT
Technical

7. PERIOD COVERED *(Inclusive Dates)*

8. PERFORMING ORGANIZATION - NAME AND ADDRESS *(If NRC, provide Division, Office or Region, U.S. Nuclear Regulatory Commission, and mailing address; if contractor, provide name and mailing address.)*
KTH
Division of Nuclear Power Safety
AlbaNova University Center, Roslagstullsbacken 21
SE-106 91 Stockholm, Sweden

9. SPONSORING ORGANIZATION - NAME AND ADDRESS *(If NRC, type "Same as above"; if contractor, provide NRC Division, Office or Region, U.S. Nuclear Regulatory Commission, and mailing address.)*
Division of Systems Analysis
Office of Nuclear Regulatory Research
U.S. Nuclear Regulatory Commission
Washington, DC 20555-0001

10. SUPPLEMENTARY NOTES
A. Calvo, NRC Project Manager

11. ABSTRACT *(200 words or less)*
The project aims to (1) conduct the validation of thermal-hydraulics codes RELAP5 Mod 3.3 Patch 03 and TRACE v5.0 Patch 2 on the critical flow experiment giving comprehensive knowledge about the codes' behavior; (2) provide information about sensitivity impact of user-defined variables of critical two-phase models implemented into the codes; (3) and to obtain statistical data for variety of length-to-diameter L/D ratios of pipe. The experimental set-up consisted of vessel, discharge pipe and the group of test nozzles. The vessel was 24.5 m high, with internal average diameter of 5.2 m. The discharge pipe was 6.308 m long with internal diameter of 0.72 m. A total number of nine nozzles was used in the experiment and is characterized by L/D ratios of 0.3, 1.0, 1.5, 1.7, 3.0, 3.1, 3.6 and 3.7. The main conclusions of the studies are that for Marviken Critical Flow Test (CFT) (i) RELAP5 Henry-Fauske model gives more accurate results than RELAP5 Ransom-Trapp (R-T) model; (ii) TRACE R-T gives better results than RELAP5 R-T; and (iii) the dependence between length-to-diameter L/D ratio of the nozzle and the calculation's accuracy has not been observed.

12. KEY WORDS/DESCRIPTORS *(List words or phrases that will assist researchers in locating the report.)*
Marviken
critical flow
two-phase flow
RELAP5
TRACE
Henry-Fauske
Ransom-Trapp

13. AVAILABILITY STATEMENT
unlimited

14. SECURITY CLASSIFICATION
(This Page)
unclassified
(This Report)
unclassified

15. NUMBER OF PAGES

16. PRICE

Federal Recycling Program

UNITED STATES
NUCLEAR REGULATORY COMMISSION
WASHINGTON, DC 20555-0001

OFFICIAL BUSINESS

NUREG/IA-0401

Assessment of Two-Phase Critical Flow Models Performance in RELAP5 and TRACE Against Marviken Critical Flow Tests

February 2012